Swiss Finance Institute
Research Paper Series N°12 - 23

Time-Changed Lévy LIBOR Market Model: Pricing and Joint Estimation of the Cap Surface and Swaption Cube

Markus LEIPPOLD
University of Zurich and Swiss Finance Institute

Jacob STROMBERG
University of Zurich and Swiss Finance Institute (PhD Program)

swiss:finance:institute

FINRISK
National Centre of Competence in Research
Financial Valuation and Risk Management

Electronic copy available at: http://ssrn.com/abstract=2065375

swiss:finance:institute

Established at the initiative of the Swiss Bankers' Association, the Swiss Finance Institute is a private foundation funded by the Swiss banks and Swiss Stock Exchange. It merges 3 existing foundations: the International Center FAME, the Swiss Banking School and the Stiftung "Banking and Finance" in Zurich. With its university partners, the Swiss Finance Institute pursues the objective of forming a competence center in banking and finance commensurate to the importance of the Swiss financial center. It will be active in research, doctoral training and executive education while also proposing activities fostering interactions between academia and the industry. The Swiss Finance Institute supports and promotes promising research projects in selected subject areas. It develops its activity in complete symbiosis with the NCCR FinRisk.

The National Centre of Competence in Research “Financial Valuation and Risk Management” (FinRisk) was launched in 2001 by the Swiss National Science Foundation (SNSF). FinRisk constitutes an academic forum that fosters cutting-edge finance research, education of highly qualified finance specialists at the doctoral level and knowledge transfer between finance academics and practitioners. It is managed from the University of Zurich and includes various academic institutions from Geneva, Lausanne, Lugano, St.Gallen and Zurich. For more information see www.nccr-finrisk.ch .

This paper can be downloaded without charge from the Swiss Finance Institute Research Paper Series hosted on the Social Science Research Network electronic library at:

http://ssrn.com/abstract=2065375

FNSNF Swiss National Science Foundation

FINRISK National Centre of Competence in Research Financial Valuation and Risk Management

Electronic copy available at: http://ssrn.com/abstract=2065375

Time-Changed Lévy LIBOR Market Model: Pricing and Joint Estimation of the Cap Surface and Swaption Cube

Markus Leippold[a,*], Jacob Strømberg[a]

[a]*Department of Banking and Finance, University of Zurich, Switzerland and Swiss Finance Institute (SFI)*

Abstract

We propose a novel time-changed Lévy LIBOR market model for the joint pricing of caps and swaptions. The time changes are split into three components. The first component allows us to match the volatility term structure, the second generates stochastic volatility, and the third one accommodates for stochastic skew. The model is parsimonious, yet flexible enough to accommodate the behavior of both caps and swaptions well. For the joint estimation we use a comprehensive dataset spanning the recent financial crisis. We find that, even during the recent financial crisis, neither market is as fragmented as suggested by the previous literature.

JEL classification: C51, E43, G13.

Keywords: LIBOR market models; time-changed Lévy process; caps volatilities; swaption cube; unscented Kalman filter.

We thank G. William Schwert (the editor), Marc Chesney, Fabio Mercurio, Fabio Trojani, and Thomas T. Kristensen from Nykredit for providing access to skew data on implied swaption volatilities. Financial support from the Swiss Finance Institute (SFI), Bank Vontobel, and the National Center of Competence in Research "Financial Valuation and Risk Management" is gratefully acknowledged. Finally, we are especially grateful for the detailed feedback of an anonymous referee. Any remaining errors are ours.

*Corresponding author. Tel:+41 (0)44 634 5069.
E-mail address: markus.leippold@bf.uzh.ch (M. Leippold).

Electronic copy available at: http://ssrn.com/abstract=2065375

1. Introduction

We introduce a novel time-changed Lévy LIBOR market model (LMM) that is analytically tractable and parsimonious. Yet, it is flexible enough to jointly and consistently price caps and swaptions in an efficient way. For the period spanning the recent financial crisis, we perform a comprehensive empirical analysis of our model. We make use of a unique data set of implied volatilities of the cap surface and the entire swaption cube. The swaption cube refers to the implied volatilities of swaptions indexed by the expiry date of the option, the strike rate, and the tenor of the underlying swap. While previous endeavors on the joint pricing of caps and swaptions restrict their swaption data to at-the-money (ATM) quotes,[1] we incorporate all information contained in non-ATM volatilities for estimating the model.[2] To our best knowledge, this is the first paper that develops and estimates a model that jointly prices the whole swaption cube and the caps implied volatility surface.

To design our theoretical model, we start with a preliminary data analysis of the cap volatility surface and the swaption cube. We then introduce three distinct model devices to match the stylized features of the data. The first component is a Brownian motion combined with a parametric function, which allows us to capture the volatility term structure. The second component is a time-changed Brownian motion that generates stochastic volatility. Correlating the time change with the changes in the LIBOR rate gives us additional flexibility to match implied volatility skews. The third component is a time-changed jump process with asymmetric upward and downward jumps. This component allows us to accommodate variations in volatility skews over time. Hence, these three components not only match different characteristics of the implied volatilities, but also allow for a parsimonious parameterization. The parsimony is crucial for both efficient pricing and model estimation.

The modeling approach we take belongs to the general class of time-changed Lévy processes. Our motivation to use this class[3] lies in its generality. On the one hand, Lévy processes can generate almost any return innovation distribution and they can account for potential discontinuities in

[1] See, e.g., Jarrow, Li, and Zhao (2007).

[2] Data on the swaption cube have not been available to researchers until recently. To our knowledge, Trolle and Schwartz (2012) are the first to systematically analyze data from the swaption cube.

[3] Lévy models, but without time changes have been adopted for modeling interest rates within the class of LMMs by, e.g., Eberlein and Raible (1999), Eberlein and Ozkan (2005), Eberlein and Kluge (2006), and Eberlein and Liinev (2007).

the LIBOR rate dynamics.[4] On the other hand, applying time changes randomizes the innovation distribution of LIBOR rates over time. Imposing suitable time changes allows us to match volatility term structure effects, to generate stochastic volatility, and to accommodate for stochastic skew. While the literature on Lévy term structure models has been exclusively concerned with presenting a theoretically consistent no-arbitrage framework for pricing derivatives, no guidance has been given on the empirical performance of these models. We fill this gap and bring our time-changed Lévy model to the data.

We estimate our model using a maximum likelihood method joint with the unscented Kalman filter. Analyzing our parameter estimates, we find a strong negative correlation between changes in volatility and changes in LIBOR rates. This negative correlation may be driven by hedging activities in the market for mortgage backed securities (MBS). Previous literature argues that, as interest rates drop and borrowers prepay their mortgages, the increasing hedging activity of government sponsored institutions, such as Fannie Mae and Freddie Mac, may lead to an increase in interest rate volatilities, particularly for longer maturities.[5]

To examine whether the markets of caps and swaptions are integrated during the recent financial crisis, we carefully analyze the characteristics of the pricing errors. Our empirical analysis suggests that caps and swaptions markets are well integrated during the financial crisis, especially when we look at contracts with intermediate and longer maturities. In contrast, several papers[6] find segmentation between the two markets. Such findings are more likely driven by the rigidity of the model used, because our parsimonious and yet flexible model can accommodate the variations of the two markets very well.

We proceed as follows. In Section 2, we describe the data and present a preliminary data analysis on the implied volatilities of caps and the swaption cube, which guided our model design. We introduce the time-changed Lévy LIBOR model in Section 3 and show how to construct the family of forward LIBOR and swap rates. In Section 4, we adopt the fast Fourier transform (FFT)

[4]Indeed, several papers have empirically documented the need for incorporating jumps in interest rates, e.g., Babbs and Webber (1997), Das (2002), El-Jahel, Lindberg, and Perraudin (1997), and Johannes (2004).

[5]Duarte (2008) showed that the inclusion of prepayment speed as an additional factor in the LIBOR model of Longstaff, Santa-Clara, and Schwartz (2001) significantly reduces the pricing error of ATM swaptions. These results have been further corroborated by Li and Zhao (2009). However, hedging demand from the MBS market may have decreased when on January 5, 2009, the Fed began purchasing fixed rate mortgage backed securities guaranteed by Fannie Mae, Freddie Mac, and Ginnie Mae.

[6]See, e.g., Jagannathan, Kaplin, and Sun (2003), Longstaff, Santa-Clara, and Schwartz (2001) , Brigo and Mercurio (2002), Driessen, Klaassen, and Melenberg (2003), and Fan, Gupta, and Ritchken (2003).

technique to price interest rate derivatives within our Lévy framework. In Section 5, we present our estimation strategy based on the unscented Kalman filter. In Section 6, we present the results of our estimation exercise and Section 7 concludes.

2. Data analysis

We obtain the cap/floor implied volatility mid-quotes on the U.S. dollar three-month forward LIBOR rate from Bloomberg (ICAP), covering a wide range of strikes and maturities. The implied volatility quotes are available for ten fixed maturities that include every year from one to ten years. At each date and maturity, we have seven fixed strike levels, including 1.5, two, three, four, five, six, and seven percent, and also one floating strike level at the money. We obtain the swaptions implied volatility data from BGC Partners.[7] The ATM swaption quotes were collected for option maturities equal to three and six months, and one, two, three, four, five, seven, and ten years. These option maturities are combined with swap terms of one, two, three, four, five, seven, and ten years. We end up with a total of 63 ATM swaptions implied volatility quotes per observation day. For out-of-the-money and in-the-money volatilities, we collect option maturities equal to three months, one year, five years, and ten years. These option maturities are combined with swap terms of two, five, and ten years, spanning strikes of $\pm\{25, 50, 100, 200\}$ basis points away from the ATM swaption quotes.

Our dataset spans the period from August 8, 2007 to August 11, 2010, covering three years of data. This period spans the core period of the recent financial crisis and thus serves as an interesting period over which to test our model. For the estimation period, we consider weekly data sampled on Wednesdays to avoid weekday effects. The summary statistics of the LIBOR and swap rates are well documented. Therefore, we focus on the behavior of the cap/floor and swaptions implied volatility quotes along three important dimensions: moneyness, maturity (of the option as well as the swap), and time.

When we estimate our model, we follow other studies on pricing interest rate derivatives (e.g., Jarrow, Li, and Zhao (2007)) and define the moneyness of a contract as the ratio between the strike

[7] BGC Partners, Inc. (BGC) is a leading global intermediary for wholesale financial markets, specializing in brokering a broad range of financial products, including fixed income and interest rates. For a further description of the swaption cube, including liquidity issues, refer to Trolle and Schwartz (2012).

and the ATM strike of the particular contract (cap or swaption). For caps we consider moneyness spanning from 0.80 to 1.20 with intervals of 0.10. For swaptions, due to lower liquidity in the cross-section, we consider a range of moneyness from 0.90 to 1.10 with intervals of 0.05. In total, we end up with 161 interest rate derivative quotes (50 cap/floor and 111 swaption quotes) spanning three years of data (158 weeks) which yields a total of $25,438$ quotes to be matched in the joint estimation.

2.1. Time-series dynamics of the implied volatilities of ATM caps and swaptions

Figure 1 shows the evolution of the implied volatilities of ATM caps and swaptions spanning our data sample period. There is significant time-variation in the implied volatilities for both caps and swaptions. From levels of around 20% before the crisis, the implied volatilities increased dramatically, reaching levels above 100% for the shorter-dated option maturity contracts. Since implied volatilities are quoted under Black (1976)'s model, which assumes log-normally distributed forward LIBOR/swap rates, this increase may not only the effect of markets being more volatile, but also a derived effect of interest rates going down.

[Figure 1 about here.]

The implied volatilities in the two markets exhibit similar co-movements over time. This behavior is natural since caps and swaptions share essentially the same underlying. The forward swap rates driving swaption prices can be viewed as a weighted sum of forward LIBOR rates, which drive cap prices. Indeed, the correlation of the one year caps and swaptions ATM implied volatilities is 95% over our sample period. Furthermore, the average correlation between the ATM implied volatilities of caps and swaptions across all option and swap maturities averages 84%. However, the correlation decreases with increasing maturity of the underlying swap. Hence, swaps with longer maturities carry some term structure information that is not contained in the LIBOR rate underlying the cap prices. Nevertheless, the strong co-movement at shorter swap maturities suggests these two markets should be analyzed jointly, as they may be significantly integrated.

2.2. Volatility term structure across option maturities

When we analyze swaption data, we have two different maturity dimensions: the maturity of the option contract and the maturity or tenor of the underlying swap. We only discuss the option maturity dimension and keep the swap tenor fixed.

[Figure 2 about here.]

In Figure 2, we plot the evolution of the volatility term structure for ATM caps (Panel A) and for ATM swaptions on a one year swap (Panel B). During our sample period, the term structure of volatilities is usually monotonically decreasing for both caps and swaptions. Also, the term structure for caps tends to be higher than for swaptions. However, both curves exhibit from time to time a hump-shaped term structure. Hence, term structure shapes for both markets may simultaneously share similar patterns through time. If this is indeed the case, then the joint estimation using data from both markets may facilitate identification of the model.

2.3. Cap and swaptions implied volatility smile/skew across moneyness

For our graphical analysis of implied volatilities across moneyness, we use a quadratic fit to the quoted implied volatilities, for which we standardize the moneyness d by

$$d \equiv \frac{\ln K/S(t,T)}{ATMV(t,T)\sqrt{T-t}}, \tag{1}$$

where K is the strike rate level of the cap/swaption, $S(t,T)$ denotes the swap rate of the corresponding maturity (spot for caps and forward starting for swaptions), $ATMV(t,T)$ is the ATM implied volatility quote, and $T-t$ denotes the option's time-to-maturity. Since the cap is a portfolio of caplets, the moneyness for different caplets differs due to differences in both maturities and underlying forward rates. Hence, for caps, the above definition of moneyness represents an aggregate approximate measure. We perform a quadratic fit as follows,

$$IV = \widehat{a} + \widehat{b}\, d + \widehat{c}\, d^2 + \epsilon. \tag{2}$$

The slope estimate $\widehat{b}$ measures the implied skewness, while the curvature estimate $\widehat{c}$ captures the implied kurtosis in the distribution of the underlying rate. The estimate $\widehat{a}$ captures the average

level of the implied volatilities and ϵ denotes the residual between the actual implied volatility quotes and the quadratic fit.

[Figure 3 about here.]

Figure 3 plots the caps and swaptions implied volatility smiles and skews at an arbitrary day together with their average shapes. On November 28, 2007 (Figure 3, Panels A and B), the implied volatilities exhibit significant skewness at each maturity. Note that November 28, 2007 is just at the onset of the financial crisis. At the time, there was significant uncertainty about the current and future levels of the forward LIBOR rate, which drives the amount of interbank lending. The relatively high caps implied volatilities for low strikes indicate that financial institutions were demanding caps with low strikes, presumably as an insurance or hedge against future hikes in the LIBOR.

A similar pattern, although to a lesser extent, emerges in Panel B for swaption prices. Here, we plot the implied volatilities for swaptions on the five year swap. These volatilities are quoted at a lower level than the corresponding volatilities for caps, which corresponds to the intuition that the LIBOR rate underlying the cap should be more volatile than the swap rate, as it has a shorter maturity (three months). Nevertheless, it seems that on that particular day, both markets shared the same qualitative characteristics in terms of the volatility shape. This observation is confirmed when we look at the average shapes of the implied volatilities across moneyness in Panels C and D of Figure 3. They are all negatively skewed for both markets. The cap volatilities are higher on average than the swaption volatilities. Furthermore, they tend to have a more pronounced skew and, at least for the caps volatilities with one year maturity, the implied volatility has a slight smile pattern.

2.4. Dynamic properties of the term structure of the caps and swaptions implied skew and curvature

For our model design, we may gain further insights into the properties of caps and swaptions dynamics by analyzing the slope and curvature of the implied volatilities over time. As in the previous section, we summarize each caps and swaptions implied volatility smile by three quantities:

its level $\widehat{a}$, its slope $\widehat{b}$, and its curvature $\widehat{c}$ from the quadratic fit in equation (2) normalized by the ATM volatility level.

[Figure 4 about here.]

In Figure 4, we plot the time series behavior of the slope and curvature of caps and swaptions implied volatility for an option maturity of five years. For the underlying swap, we choose a tenor of two years. Panel A shows a cap volatility skew that is systematically higher than the swaption skew. Nevertheless, they move in the same direction. Hence, we can conclude that both the forward rate as well as the swap rate exhibit negative skewness and that their skewness is highly correlated.

By inspection of Panel B, we find that the curvature behaves slightly differently. At the beginning of the sample period, the curvature of the caps is lower than that of the swaptions. In particular, the time series plot indicates that the forward rates did not have much excess kurtosis until January 2008. In the subsequent period, the excess kurtosis increased steadily to levels similar to the excess kurtosis of the two year swap rate. Furthermore, the variation in the caps' curvature, and hence in the forward rate's excess kurtosis, is much more pronounced. Nevertheless, the curvature for the implied volatilities of caps and swaptions seems to be correlated as well. Repeating the same calculations across different option maturities, swap tenors, and moneyness, we observe that the correlations between skew and curvature are substantial, especially for intermediate and long option maturities.

Hence, by incorporating information from the whole swaption cube, we do not necessarily have to introduce a large number of additional factors to fully capture the moneyness and the two maturity dimensions. Instead, given the high co-movement especially across the maturity dimensions, the swaption cube might improve the model identification when it comes to estimation.

2.5. Principal component analysis

Now that we have analyzed the data across different maturities and levels of moneyness, the next step is to analyze how many factors are needed to jointly describe the caps and swaptions data in the cross-sectional and time-series dimension. We do so by using a principal component analysis

(PCA). As in Heidari and Wu (2003),[8] we first perform a PCA of the LIBOR and swap rates to identify the common factors driving the yield curve. Once we have extracted the common factors from the interest rate market, we regress the caps and swaptions implied volatilities on the yield curve factors. We use the regression residuals to perform another PCA to identify the common factors driving the implied volatilities. Finally, we regress the caps and swaptions implied volatilities on both the yield curve and the common volatility factors.

[Table 1 about here.]

Table 1 shows the resulting R^2 values. Since we have in total 161 time series of implied volatilities, we take averages across caps, ATM swaptions, and non-ATM swaptions. We analyze different factor combinations (m, n), where m is the number of yield curve factors and n is the number of volatility factors. On average, a model with one term structure and one volatility factor already explains 88.5% of the variance in caps and swaptions implied volatilities. However, especially for non-ATM swaptions, models that do not include more than three factors cannot explain more than 90% of the variation. When we add additional factors, the explained variation for all implied volatilities increases well above 93%. The $(3, 3)$-model with three term structure and three volatility factors explains 97%. This result is very close to the findings in Heidari and Wu (2003). However, they analyze only ATM swaptions data.

We also see from Table 1 that the $(3, 2)$-model with three term structures and two volatility factors does a reasonably good job in explaining the variation across the different markets. The total variation explained is above 96% and for non-ATM swaptions close to 95%. Therefore, for the sake of parsimony, we content ourselves with designing a model that is based on two instead of three volatility factors. To further validate such a factor structure, we can break down the explained variation across the different caps and swaptions implied volatilities for the $(3, 2)$-model. Since this model already explains 97.7% of the variation in caps implied volatilities, in Table 2, we only present the results for the swaptions volatilities.

[Table 2 about here.]

[8] Note, however, that we do not introduce their modification to explicitly account for the sharp difference in liquidities between the interest rate market and the swaptions market.

Table 2 shows the R^2 values for swaptions across different option maturities and swap tenors (Panel A) and across different levels of moneyness (Panel B). For the ATM swaptions in Panel A, we find the comforting result that all entries are above 90%. The performance of the $(3, 2)$-model struggles most for the ten year option maturity with some values only slightly above 90%. We also note that the R^2 values are more stable across swap tenors than across option maturities, which indicates that the volatility factors may act differently mainly along the option maturity dimension, while their impact along the swap tenor dimension is relatively flat. Again, this observation is in line with Heidari and Wu (2003). For the non-ATM swaptions in Panel B, we find a similar pattern. For a given level of moneyness and if compared across option maturities, the variation of the R^2 values is larger than the variation of R^2 values across swap tenors. However, even for non-ATM swaptions, the R^2 values never fall below 90% for the $(3, 2)$-model.

3. The specification of the Lévy LIBOR market model

Guided by the stylized features of the caps' implied volatility surface and the swaption cube, we next introduce our term structure model. Rather than starting from instantaneous forward rates or zero-coupon bond prices, we begin directly with the specification of the forward LIBOR rates and model them as Lévy processes. To describe the tenor structure of the forward LIBOR rates, we consider a fixed set of increasing and equidistant maturities $T_0, T_1, \ldots, T_n$ with $\delta \equiv T_{j+1} - T_j$ for all j. The maturity T_n denotes the terminal maturity and the tenor δ is typically three months. We assume the existence of an initial strictly positive and decreasing term structure of zero-coupon bonds, $P(0, T)$, for $T \in (0, T_n]$. We denote by $L(0, T_j) \equiv L(0; T_j, T_{j+1})$ the forward LIBOR rate contracted at date $t = 0$ for the period $[T_j, T_{j+1}]$ defined by

$$L(0, T_j) \equiv \frac{1}{T_{j+1} - T_j} \left(\frac{P(0, T_j)}{P(0, T_{j+1})} - 1 \right), \quad j = 0, \ldots, n-1. \tag{3}$$

3.1. Model design

We consider a complete filtered probability space $\{\Omega, \mathcal{F}_{T_n}, (\mathcal{F}_t)_{0 \le t \le T_n}, \mathbb{P}\}$ with the augmented filtration $(\mathcal{F}_t)_{0 \le t \le T_n}$ satisfying the usual conditions. As it is convenient to price interest rate derivatives under the so-called T-forward measure $\mathbb{Q}_n \sim \mathbb{P}$, we specify the dynamics of the forward LIBOR

rate directly under $\mathbb{Q}_n$. Under this measure, $L(t, T_{n-1})$ is a martingale on the interval $[0, T_{n-1}]$ and we assume that it has the representation

$$L(t, T_{n-1}) = L(0, T_{n-1}) \exp\left(\int_0^t b^{\mathbb{Q}_n}(s, T_{n-1}, T_n) ds + \int_0^t dX_s \right), \tag{4}$$

where

$$\begin{aligned} X_s = & \int_0^t \lambda(s, T_{n-1}) dB_s^{\mathbb{Q}_n} + \int_0^t \sqrt{V_s^W} dW_s^{\mathbb{Q}_n} + \int_0^t \int_{-\infty}^0 x \left(\mu^-(ds, dx) - \pi_{J^-}^{\mathbb{Q}_n}(x) dx \nu_s^J ds \right) \\ & + \int_0^t \int_0^\infty x \left(\mu^+(ds, dx) - \pi_{J^+}^{\mathbb{Q}_n}(x) dx \nu_s^J ds \right) \end{aligned} \tag{5}$$

is a non-homogeneous Lévy process. The term $b^{\mathbb{Q}_n}(t, T_{n-1}, T_n)$ in (4) denotes a deterministic drift, which we need to specify in such a way that the forward LIBOR rate $L(t, T_{n-1})$ becomes a $\mathbb{Q}_n$-martingale. We decompose the random shocks in the above forward LIBOR rate dynamics into different types. First, we introduce continuous shocks by two standard Brownian motions $B_t^{\mathbb{Q}_n}$ and $W_t^{\mathbb{Q}_n}$, for which we assume $dB_t^{\mathbb{Q}_n} dW_t^{\mathbb{Q}_n} = 0$. Second, we introduce discontinuous shocks J_t, for which we allow a separate specification of positive jumps J_t^+ and negative jumps J_t^-, i.e., $J_t = J_t^+ + J_t^-$. By $\mu^-(dt, dx)$ and $\mu^+(dt, dx)$, we denote the counting measures for upward and downward jumps, respectively. By $\pi_{J^+}^{\mathbb{Q}_n}(x)$ and $\pi_{J^-}^{\mathbb{Q}_n}(x)$, we denote the corresponding Lévy densities, which characterize the jump structure under $\mathbb{Q}_n$. The arrival rate of upward jumps of size x at time t is governed by $\pi_{J^+}^{\mathbb{Q}_n}(x)\nu_t^J$. Hence the $\mathbb{Q}_n$-compensator for upward jumps becomes $\pi_{J^+}^{\mathbb{Q}_n}(x) dx \nu_t^J dt$. The compensator for downward jumps has the same form, but with $\pi_{J^+}^{\mathbb{Q}_n}(x)$ replaced by $\pi_{J^-}^{\mathbb{Q}_n}(x)$.[9]

3.1.1. Time changes

The specification of the LIBOR rate in (4) and (5) is a non-homogenous Lévy process under $\mathbb{Q}_n$, defined by its time-dependent local characteristic triplet. This time dependency can also be interpreted through the following time changes:

$$\mathcal{T}_t^B = \int_0^t \lambda(s, T_{n-1})^2 ds, \qquad \mathcal{T}_t^W = \int_0^t V_s^W ds, \qquad \mathcal{T}_t^J = \int_0^t \nu_s^J ds. \tag{6}$$

[9] A similar specification of the jump components has recently been proposed by Carr and Wu (2008) for modeling equity index options.

We can specify these three components separately. First, we specify the time changes $\mathcal{T}_t^W$ and $\mathcal{T}_t^J$ through their activity rates under $\mathbb{Q}_n$:

$$\begin{aligned} dV_t^W &= \kappa_W(\theta_W - V_t^W)dt + \sigma_W\sqrt{V_t^W}d\widetilde{W}_t^{\mathbb{Q}_n}, \qquad dW_t^{\mathbb{Q}_n}d\widetilde{W}_t^{\mathbb{Q}_n} = \rho dt, \\ d\nu_t^J &= \kappa_J(\theta_J - \nu_t^J)dt + \sigma_J\sqrt{\nu_t^J}dZ_t^{\mathbb{Q}_n}, \end{aligned} \tag{7}$$

where $\widetilde{W}_t^{\mathbb{Q}_n}$ and $Z_t^{\mathbb{Q}_n}$ are $\mathbb{Q}_n$-Brownian motions. We assume that the instantaneous correlation between the time changes of the jump and the continuous component is zero. The specification in (7) dictates that stochastic volatility enters our model via two different sources: (i) the time change of the Brownian motion $W_t^{\mathbb{Q}_n}$ and (ii) the stochastic activity rate of jumps ν_t^J. Furthermore, to account for a potential leverage effect, we allow the instantaneous correlation between the activity rate V_t^W and the Brownian motion $W_t^{\mathbb{Q}_n}$ to be nonzero.

In addition to the time changes $\mathcal{T}_t^W$ and $\mathcal{T}_t^J$, we also introduce a purely deterministic time change $\mathcal{T}_t^B$ governed by the parametric functional form of $\lambda(t, T_{n-1})$. By choosing a functional form such as

$$\lambda(t, T_{n-1}) = (\beta_1 + \beta_2(T_{n-1} - t))\exp(-\beta_3(T_{n-1} - t)) + \beta_4, \tag{8}$$

we can ensure not only sufficient flexibility for the volatility function to match potentially hump-shaped patterns (see, e.g., Rebonato, McKay, and White (2009)), but also analytical tractability.[10]

3.1.2. Jump process

For the jump specification, we borrow the variance-gamma jump process from Carr and Wu (2007). They propose a simple yet flexible specification for the Lévy density that successfully reconciles the properties of currency option skews. We split the Lévy density under the terminal forward measure $\mathbb{Q}_n$ into a right-skewed jump component and a left-skewed jump component:

$$\pi_J^{\mathbb{Q}_n}(x) = \begin{cases} \pi_{J^+}^{\mathbb{Q}_n}(x) = \lambda e^{-\frac{x}{\nu_+}}x^{-1}, & x > 0 \\ \pi_{J^-}^{\mathbb{Q}_n}(x) = \lambda e^{-\frac{|x|}{\nu_-}}|x|^{-1}, & x < 0 \end{cases}, \tag{9}$$

where $\lambda, \nu_+, \nu_- > 0$. Hence, we let the jump arrival rate decrease monotonically with increasing jump size. The parameters ν_+ and ν_- control the scale of the positive and negative jumps. Applying

[10] Note that $\lim_{t\to T}\lambda(t,T) = \beta_1 + \beta_4$ and $\lim_{T\to\infty}\lambda(t,T) = \beta_4$. Furthermore, the maximum of the volatility curve occurs at a T^*, where $T^* = 1/\beta_3 - \beta_1/\beta_2$.

different scales allows us to capture any asymmetric discontinuous movements in the jump arrival rate of the forward LIBOR rate. Because the characteristic exponent of the jump process in (9) is available in closed form, our LIBOR model is still analytically tractable.

Before we continue with constructing the family of forward LIBOR and swap rates, we remark that our additive structure not only ensures the analytical tractability of the characteristic exponent of the underlying Lévy process, which is crucial for deriving our pricing formulae, but the explicit mapping of the various components, to capture specific properties of caps and swaptions implied volatilities, also facilitates the economic interpretation of the model. First, we have seen in the preliminary data analysis of Section 2, that we need a time-varying stochastic volatility in the underlying LIBOR forward rate (see Figure 1). We let the process V_t take care of this. Second, as Figure 2 illustrates, we also need a sufficiently general and flexible volatility function to capture various shapes of the volatility term structure, such as monotonically decreasing and hump-shaped forms. Therefore, we have chosen the functional form of $\lambda(t,T)$ as in equation (8). Third, Figure 3 provides evidence for implied volatility smiles/skews in both the caps and swaptions market, underscoring the importance of allowing for a non-zero correlation between innovations to the forward rates and its underlying stochastic volatility.[11] Fourth, the findings in Figure 4 call for a model that can match both the persistent fat-tail behavior and the strong time variation in the skewness (specifically for short option maturities) of the forward-neutral distribution of the log-LIBOR forward rate. The fat-tail behavior may be captured by including a jump component into the underlying forward rate dynamics. As Carr and Wu (2007) remark, standard jump-diffusion models (e.g., Merton (1976) type models) have difficulty in generating strong time variation in the risk-neutral skewness. By randomizing the clock for the Lévy jump component as we do in our model specification, we can introduce stochastic skewness into the underlying distribution of the log-LIBOR forward rate. Finally, the principal component analysis indicates that our model specification should be rich enough to match the data across the dimensions of the option maturity, the swap tenor, and the moneyness in both the caps and swaptions market. Hence, while keeping the model parsimonious with three term structure factors and two volatility factors, each model device has its own role in matching the stylized facts of caps and swaptions volatilities.

[11] See also Casassus, Collin-Dufresne, and Goldstein (2005).

3.1.3. Market price of risk

To capture the observed time series dynamics under the historical measure (represented by $\mathbb{P}$), we need to specify the different market prices of risk related to each stochastic component in our model. However, because the forward LIBOR and swap rate processes under the measure $\mathbb{P}$ are not relevant for option pricing, we leave the market price of return risk unspecified and focus on the activity rate processes. For simplicity, we assume constant market prices of risk for the activity rates. In particular, we define the measure change from the terminal forward LIBOR measure $\mathbb{Q}_n$ to $\mathbb{P}$ by

$$\frac{d\mathbb{P}}{d\mathbb{Q}_n\,|_{\mathcal{F}_t}} = \mathcal{E}\left(-\gamma^V \widetilde{W}_{\mathcal{T}_t^W}\right)\mathcal{E}\left(-\gamma^\nu Z_{\mathcal{T}_t^J}\right). \tag{10}$$

3.2. Constructing the family of forward LIBOR rates

In the representation of the forward LIBOR rate $L(t,T_{n-1})$ in equations (4) and (5), the deterministic term $b^{\mathbb{Q}_n}(t,T_{n-1},T_n)$ corresponds to a convexity-adjustment related to the Brownian motions and to the jump components, respectively. For any $j=0,1,\ldots,n-1$, $L(t,T_j)$ has to be a martingale under the T_{j+1}-forward measure $\mathbb{Q}_{j+1}$, which we can ensure by a corresponding adjustment of the term $b^{\mathbb{Q}_{j+1}}(t,T_j,T_{j+1})$. The proposition below shows how this martingale property can be enforced.[12]

Proposition 1. *The forward LIBOR rate $L(t,T_j)$ is a martingale under the T_{j+1}-forward measure for $j=0,\ldots,n-1$ if the following drift condition is satisfied:*

$$b^{\mathbb{Q}_{j+1}}(t,T_j,T_{j+1}) = -\frac{1}{2}\lambda^2(t,T_j) - \frac{1}{2}V_t^W - \int_{-\infty}^{\infty}(e^x-1-x)\,\pi_J^{\mathbb{Q}_{j+1}}(dx)\nu_t^J.$$

Proposition 1 allows us to express the martingale dynamics of the forward LIBOR rate $L(t,T_j)$ under the T_{j+1}-forward measure by

$$\begin{aligned}\frac{dL(t,T_j)}{L(t,T_j)} &= \lambda(t,T_j)dB_t^{\mathbb{Q}_{j+1}} + \sqrt{V_t^W}dW_t^{\mathbb{Q}_{j+1}} + \int_{-\infty}^{0}(e^x-1)\left(\mu^-(dt,dx) - \pi_{J^-}^{\mathbb{Q}_{j+1}}(x)dx\nu_t^J dt\right)\\ &+ \int_0^{\infty}(e^x-1)\left(\mu^+(dt,dx) - \pi_{J^+}^{\mathbb{Q}_{j+1}}(x)dx\nu_t^J dt\right),\end{aligned} \tag{11}$$

subject to the activity rate processes in equations (6)–(8) and the jump specification given in equation (9) under the appropriate forward measure.

[12] We relegate all proofs to Appendix A.

For a recursive backward construction of the family of forward LIBOR rates $L(t,T_j)$ under their corresponding forward measures $\mathbb{Q}_{j+1}$, we have to switch between different forward measures. For that purpose, we need to know how the components of the non-homogenous Lévy process X_t must be adjusted for different forward measures. Proposition 2 tells us how to do so.[13]

Proposition 2. *For each $j = 2,\ldots,n$, the forward measure defining the martingale dynamics of the family of forward LIBOR rates is related to the terminal forward measure $\mathbb{Q}_n$ by*

$$dB_t^{\mathbb{Q}_{j-1}} = dB_t^{\mathbb{Q}_n} - \sum_{k=1}^{n+1-j} \frac{\delta L(t,T_{n-k})}{\delta L(t,T_{n-k})+1}\lambda(t,T_{n-k})dt \tag{12}$$

$$dW_t^{\mathbb{Q}_{j-1}} = dW_t^{\mathbb{Q}_n} - \sum_{k=1}^{n+1-j} \frac{\delta L(t,T_{n-k})}{\delta L(t,T_{n-k})+1}\sqrt{V_t^W}dt \tag{13}$$

$$\pi_J^{\mathbb{Q}_{j-1}}\nu_t^J = \prod_{k=1}^{n+1-j}\left(1+\frac{\delta L(t,T_{n-k})}{\delta L(t,T_{n-k})+1}\left(e^x-1\right)\right)\pi_J^{\mathbb{Q}_n}\nu^J, \tag{14}$$

where $\pi_J^{\mathbb{Q}_n}$ was defined in (9).

Next, we need to find the change of measure of the activity rate dynamics governing the stochastic volatility V_t^W that affects the Brownian motion W_t due to the non-zero correlation assumption. We present the dynamics of the activity rate process under the forward measures $\mathbb{Q}_{j+1}$ in the proposition below.

Proposition 3. *The forward changes of measure related to the Brownian motion $\widetilde{W}^{\mathbb{Q}_{j-1}}$ of the stochastic activity rate in equation* (7) *obey*

$$d\widetilde{W}_t^{\mathbb{Q}_{j-1}} = d\widetilde{W}_t^{\mathbb{Q}_n} - \sum_{k=1}^{n+1-j} \frac{\delta L(t,T_{n-k})}{\delta L(t,T_{n-k})+1}\sqrt{V_t^W}\rho dt, \quad j=2,\ldots,n. \tag{15}$$

Propositions 2 and 3 provide us with the results necessary for the construction of the family of forward LIBOR rates $L(t,T_j)_{t\in[0,T_j]}$ driven by the non-homogenous Lévy process in (5) under their corresponding forward measures $\mathbb{Q}_{j+1}$ for $j=0,\ldots,n-1$.

3.3. Constructing the family of forward swap rates

For the construction of the forward swap rates, we assume a set of equally spaced reset dates $\{T_0,T_1,\ldots,T_n\}$ with interval length δ. For a swap contract starting at date T_j, $j=1,\ldots,n-N$,

[13] For regularity conditions, we refer to Eberlein and Ozkan (2005).

the first settlement date is at time T_{j+1} and the maturity date of the swap is T_{N+j}. We fix the length N of the swap, but we let the starting date, and thus also the maturity, vary. We let $R_j^N(t) \equiv R(t; T_j, T_{j+N})$ denote the forward swap rate contracted at time t for the swap arrangement over the period $[T_j, T_{j+N}]$. In terms of zero bond prices, the swap rate equals

$$R(t; T_j, T_{j+N}) = \frac{P(t,T_j) - P(t,T_{j+N})}{\delta \sum_{k=j+1}^{j+N} P(t,T_k)} = \frac{P(t,T_j) - P(t,T_{j+N})}{S_0(T_j, T_{j+N})}, \quad j = 0, \ldots, n-N. \tag{16}$$

The numerator $S_t(T_j, T_{j+N}) = \sum_{k=j+1}^{j+N} \delta P(t,T_k)$ is often referred to as the present value of a basis point or the sliding level process.[14] In what follows, we make use of an approximate representation of the swap rate. This representation helps us retain analytical tractability.[15]

Proposition 4. *The terminal co-sliding forward swap rate $R_{n-N}^N(t)$ given by*[16]

$$R_{n-N}^N(t) \approx R_{n-N}^N(0) \exp\left(\int_0^t \sum_{k=n-N}^{n-1} \tilde{\omega}_k(0) dX_s + \textit{drift} \right), \tag{17}$$

is a $\mathbb{Q}_{n-N+1}^N$-martingale. The weights

$$\tilde{\omega}_k(0) = \frac{\omega_k(0) L(0,T_k)}{R_j^N(0)}, \tag{18}$$

with $\omega_k(0) = \frac{P(0,T_{k+1})}{\sum_{k=j+1}^{j+N} P(0,T_k)}$, are obtained by freezing the coefficients to their initial values. Under the terminal co-sliding forward swap measure $\mathbb{Q}_{n-N+1}^N$, we have

$$\begin{aligned} X_s &= \int_0^t \lambda(s,T_k) dB_s^{\mathbb{Q}_{n-N+1}^N} + \int_0^t \sqrt{V_s^W} dW_s^{\mathbb{Q}_{n-N+1}^N} + \int_0^t \int_{-\infty}^0 x \left(\mu^-(ds,dx) - \pi_{J^-}^{\mathbb{Q}_{n-N+1}^N}(x) dx \nu_s^J ds \right) \\ &\quad + \int_0^t \int_0^\infty x \left(\mu^+(ds,dx) - \pi_{J^+}^{\mathbb{Q}_{n-N+1}^N}(x) dx \nu_s^J ds \right). \end{aligned} \tag{19}$$

The jump intensity under $\mathbb{Q}_{n-N+1}^N$ becomes

$$\pi_J^{\mathbb{Q}_{n-N+1}^N}(x) \nu_s^J = e^{\varphi_2 x} \pi_J^{\mathbb{Q}_n}(x) \nu_s^J \tag{20}$$

for $J = \{J^-, J^+\}$, and the activity rate dynamics are

$$dV_t^W = \left(\kappa_W \theta_W - \tilde{\kappa}^{\mathbb{Q}_{n-N+1}^N} V_t^W \right) dt + \sigma_W \sqrt{V_t^W} d\widetilde{W}_t^{\mathbb{Q}_{n-N+1}^N} \tag{21}$$

$$d\nu_t^J = \kappa_J(\theta_J - \nu_t^J) dt + \sigma_J \sqrt{\nu_t^J} dZ_t^{\mathbb{Q}_{n-N+1}^N}, \tag{22}$$

[14] See, e.g., Bjork (2004).

[15] We use an approximation based on "freezing the coefficients" together with an approximation of exponential functions. The technique of freezing the coefficients is well established and has been tested for its quality by, e.g., Brigo and Mercurio (2006), Chapter 8. For details, refer to Appendix A.

[16] The drift in equation (17) has to be adjusted in such a way that $R_{n-N}^N(t)$ is indeed a $\mathbb{Q}_{n-N+1}^N$-martingale. As it has no impact on the pricing, we leave it unspecified.

with $\tilde{\kappa}^{\mathbb{Q}^N_{n-N+1}} = \kappa_W - \varphi_2 \sigma_W \rho$ *for a given* N*, and where* φ_2 *is defined in Lemma 2 of Appendix A.*

We remark that the above specification of the forward swap rates with fixed N is also referred to as a co-sliding forward swap rate model.[17] This specification not only facilitates the estimation and calibration of our model to actual market quotes, but most importantly, it is also consistent with our previous construction of forward LIBOR rates. Indeed, the forward LIBOR rate $L(t; T_j, T_{j+1})$ coincides with the one-period forward swap rate over the interval $[T_j, T_{j+1}]$. Hence, we can view the LIBOR market model as a sub-class of the co-sliding forward swap rate model with $N = 1$ corresponding to the three-month tenor. For a given length of the swap tenor N we can, with minimal effort, adjust all measure change results from Section 3.2 and apply them to the co-sliding forward swap rate model. In contrast, if we were to specify a swap market model based on, e.g., the co-terminal swap rate,[18] the theoretical results and the numerical implementation would become substantially more involved and cumbersome.[19]

From the specification of the co-sliding forward swap rate in Proposition 4, we can start the backward construction of the entire family of co-sliding forward swap rates. But since the co-sliding forward swap rate in (17) is an exponential of non-homogenous Lévy processes under the appropriate co-sliding forward swap rate measure, the calculations are essentially similar to those for the LIBOR model. Therefore, we omit the details of the construction of the family of co-sliding forward swap rates. The explicit calculations can be obtained from the authors on request.

4. Pricing interest rate derivatives

For pricing interest rate derivatives, we adopt the FFT technique introduced for stock options by Carr and Madan (1999).

[17] See, e.g., Musiela and Rutkowski (2005), Chapter 13.5.

[18] An example is Eberlein and Liinev (2007), who have derived measure change formulae for a Lévy swap rate model based on co-terminal forward swap rates.

[19] In a related discussion, Galluccio, Ly, Scaillet, and Huang (2007) show that the LIBOR market model is the only admissible model of a co-sliding type.

4.1. Pricing caps

A cap contract is a sum of a number of basic contracts known as caplets. Each caplet can be viewed as a call option on the underlying forward LIBOR rate such that the time-t value of the cap with maturity T_n and strike K can be represented by

$$\text{Cap}_t(K,T_n) \;=\; \sum_{j=0}^{n-1} P(t,T_{j+1})\mathbb{E}_t^{\mathbb{Q}_{j+1}}\left(\delta(L(T_j,T_j)-K)^+\right) \tag{23}$$

under the forward measure $\mathbb{Q}_{j+1}$. We can write the time-t price of a caplet on the forward LIBOR rate $L(T_j,T_j)$ with strike K and maturity T_j as

$$C_t(K,T_j) \;=\; \delta P(t,T_{j+1})\mathbb{E}_t^{\mathbb{Q}_{j+1}}\left[(L(T_j,T_j)-K)^+\right] = \delta P(t,T_{j+1})\mathbb{E}_t^{\mathbb{Q}_{j+1}}\left[(e^{Y_{T_j}}-e^k)^+\right], \tag{24}$$

where $k=\ln K$ and

$$Y_{T_j} \;=\; \ln L(t,T_j) + \int_t^{T_j} b^{\mathbb{Q}_{j+1}}(s,T_j,T_{j+1})ds + \int_t^{T_j} dX_s. \tag{25}$$

The drift $b^{\mathbb{Q}_{j+1}}(s,T_j,T_{j+1})$ is given in Proposition 1. To calculate cap prices, we make use of the complex valued measure change as developed in Carr and Wu (2004). Furthermore, for the characteristic exponent of the convexity-adjusted jump component of the Lévy process $\psi_J^{T_{j+1}}(u)$ under the measure $\mathbb{Q}_{j+1}$, we apply the widely used "freezing coefficients" approach.

Proposition 5. *The time-t price of the caplet given in* (24) *can be calculated by*

$$C_t(k,T_j) \;=\; \frac{e^{-z_i k}}{\pi}\delta P(t,T_{j+1})\int_0^\infty e^{-iz_r k}\frac{\phi_{Y_{T_j}}(z_r-iz_i-i)}{(iz_r+z_i)(iz_r+z_i+1)}dz_r.$$

The characteristic function $\phi_{Y_{T_j}}(\cdot)$ of the non-homogenous Lévy process Y_{T_j} is given by

$$\begin{aligned}\phi_{Y_{T_j}}(u) \;&=\; \mathbb{E}_t^{\mathbb{Q}_{j+1}}\left(\exp\left(iuY_{T_j}\right)\right)\\ &=\; L(t,T_j)^{iu}\exp\left[-\frac{1}{2}\left(iu+u^2\right)\int_t^{T_j}\lambda(s,T_j)^2 ds - a_W(\tau)-b_W(\tau)V_t - a_J(\tau)-b_J(\tau)\nu_t^J\right],\end{aligned}$$

where $\tau=T_j-t$ and the coefficients $a_W(\tau)$, $b_W(\tau)$, $a_J(\tau)$, and $b_J(\tau)$ are given by

$$\begin{aligned}a_i(\tau) \;&=\; \frac{\kappa_i\theta_i}{\sigma_i^2}\left[2\ln\left(1-\frac{\gamma_i-\hat\kappa_i}{2\gamma_i}\left(1-e^{-\gamma_i\tau}\right)\right)+\left(\gamma_i-\hat\kappa_i\right)\tau\right],\\ b_i(\tau) \;&=\; \frac{2\psi_i(u)\left(1-e^{-\gamma_i\tau}\right)}{2\gamma_i-\left(\gamma_i-\hat\kappa_i\right)\left(1-e^{-\gamma_i\tau}\right)}, \qquad \gamma_i=\sqrt{\hat\kappa_i^2+2\sigma_i^2\psi_i(u)}.\end{aligned}$$

For the index $i \in \{W, J\}$,

$$\psi_i(u) = \begin{cases} \psi_W(u) = \frac{1}{2}(iu + u^2) & \text{if } i = W \\ \psi_J^{\mathbb{Q}_{j+1}}(u) & \text{if } i = J \end{cases}, \qquad \hat{\kappa}_i = \begin{cases} \kappa_j^{\mathbb{M}} & \text{if } i = W \\ \kappa_J & \text{if } i = J \end{cases},$$

with $\kappa_j^{\mathbb{M}} = \kappa_W - \sum_{k=1}^{n-j-1} \frac{\delta L(t,T_{n-k})}{1+\delta L(t,T_{n-k})} \sigma_W \rho - iu\sigma_W \rho$, *and*

$$\psi_J^{\mathbb{Q}_{j+1}}(u) \approx \int_{\mathbb{R}_0} \left(1 - e^{iux}\right) \prod_{k=1}^{n-1-j} \left(1 + \frac{\delta L(t,T_{n-k})}{\delta L(t,T_{n-k}) + 1} \left(e^x - 1\right)\right) \pi_J^{\mathbb{Q}_n} dx.$$

We remark that the characteristic exponent $\psi_J^{\mathbb{Q}_{j+1}}(u)$ can be recursively calculated in closed form starting from the terminal measure $\mathbb{Q}_n$. The term $\int_t^{T_j} \lambda(s, T_j)^2 ds$ can also be calculated in closed form. Therefore, our model specification allows closed form solutions for pricing caps and floors (up to a single integration), which enables us to use FFT methods efficiently.

4.2. Pricing swaptions

A payer swaption (PS) is a call option that allows us to enter into an interest rate swap agreement at some future point in time. The term "payer" refers to the fixed leg of the contract such that, when we enter into a swap agreement, we receive the floating leg and pay the fixed leg. We consider a payer swaption on the forward swap rate $R_j^N(T_j)$ with strike K. The value under the co-sliding forward swap measure $\mathbb{Q}_{j+1}^N$ at time t is

$$\begin{aligned} PS_t(T_j, T_{j+N}, K) &= \sum_{k=j+1}^{j+N} \delta P(t, T_k) \mathbb{E}_t^{\mathbb{Q}_{j+1}^N} \left[(R_j^N(T_j) - K)^+\right] \\ &= S_t(T_j, T_{j+N}) \mathbb{E}_t^{\mathbb{Q}_{j+1}^N} \left[(R_j^N(T_j) - K)^+\right], \end{aligned} \tag{26}$$

for $j = 0, 1, \ldots, n - N$. Under the measure $\mathbb{Q}_{j+1}^N$, the forward swap rate $R_j^N(t)$ is a martingale. Since we work under the approximate swap rate derived in Proposition 4, we use the pricing formula

$$PS_t(T_j, T_{j+N}, K) \approx S_t(T_j, T_{j+N}) \mathbb{E}_t^{\mathbb{Q}_{j+1}^N} \left[\left(e^{\widetilde{Y}_{T_j}} - e^k\right)^+\right], \tag{27}$$

where $k = \ln K$ and

$$\widetilde{Y}_{T_j} = \ln R_j^N(t) + \int_0^{T_j} \sum_{k=j}^{j+N-1} \tilde{\omega}_k(t) dX_s + \textit{drift}, \tag{28}$$

and where the weights $\tilde{\omega}_k(t)$ are given in equation (18) for $t = 0$. Since the precise specification of the drift in $\widetilde{Y}_{T_j}$ matters less for the pricing formula, we simply write it as "*drift.*"[20]

Proposition 6. *The time-t price of a payer swaption with maturity T_j on the swap rate $R_j^N(T_j)$ with strike K is approximately given by*

$$PS_t(k, T_j, T_{j+N}) \approx \frac{e^{-z_i k}}{\pi} S_t(T_j, T_{j+N}) \int_0^\infty e^{-iz_r k} \frac{\phi_{\widetilde{Y}_{T_j}}(z_r - iz_i - i)}{(iz_r + z_i)(iz_r + z_i + 1)} dz_r.$$

The characteristic function $\phi_{\widetilde{Y}_{T_j}}(\cdot)$ of $\widetilde{Y}_{T_j}$ is given by

$$\begin{aligned}
\phi_{\widetilde{Y}_{T_j}}(u) &= \mathbb{E}_t^{\mathbb{Q}_{j+1}^N}\left(\exp\left(iu\widetilde{Y}_{T_j}\right)\right) \\
&= \exp\left(-\frac{1}{2}\left(iu + u^2\right)\int_t^{T_j}\left(\sum_{k=j}^{j+N-1}\tilde{\omega}_k(t)\lambda(s, T_k)\right)^2 ds\right) \times \\
&\quad R_j^N(t)^{iu}\exp\left(-a_W(\tau) - b_W(\tau)V_t - a_J(\tau) - b_J(\tau)\nu_t^J\right),
\end{aligned}$$

where $\tau = T_j - t$. The coefficients $a_W(\tau)$, $b_W(\tau)$, $a_J(\tau)$, and $b_J(\tau)$ are given by

$$\begin{aligned}
a_i(\tau) &= \frac{\kappa_i\theta_i}{\sigma_i^2}\left[2\ln\left(1 - \frac{\gamma_i - \hat{\kappa}_i}{2\gamma_i}\left(1 - e^{-\gamma_i\tau}\right)\right) + \left(\gamma_i - \hat{\kappa}_i\right)\tau\right] \\
b_i(\tau) &= \frac{2\psi_i(u)\left(1 - e^{-\gamma_i\tau}\right)}{2\gamma_i - \left(\gamma_i - \hat{\kappa}_i\right)\left(1 - e^{-\gamma_i\tau}\right)}, \qquad \gamma_i = \sqrt{\hat{\kappa}_i^2 + 2\sigma_i^2\psi_i(u)},
\end{aligned}$$

and, for the index $i \in \{W, J\}$,

$$\psi_i(u) = \begin{cases} \psi_W(u) = \frac{1}{2}(iu + u^2) & \text{if } i = W \\ \psi_J^{\mathbb{Q}_{j+1}^N}(u) & \text{if } i = J \end{cases} \qquad \hat{\kappa}_i = \begin{cases} \kappa_j^{\mathbb{M}} & \text{if } i = W \\ \kappa_J & \text{if } i = J \end{cases},$$

with $\kappa_j^{\mathbb{M}} = \kappa_W - \varphi_2\sigma_W\rho - \sum_{k=1}^{n-N-j}\frac{\delta R_{n-N+1-k}^N(t)}{1+\delta R_{n-N+1-k}^N(t)}\sigma_W\rho - iu\sigma_W\rho$. The characteristic exponents of the convexity-adjusted jump component are given by the approximation

$$\psi_J^{\mathbb{Q}_{j+1}^N}(u) \approx \int_{\mathbb{R}_0}\left(1 - e^{iux}\right)\prod_{k=1}^{n-N-j}\left(1 + \frac{\delta R_{n-N+1-k}^N(t)}{1 + \delta R_{n-N+1-k}^N(t)}\left(e^x - 1\right)\right)\pi_J^{\mathbb{Q}_{n-N+1}^N} dx,$$

where

$$\pi_J^{\mathbb{Q}_{n-N+1}^N}(x) = \begin{cases} \lambda e^{-\frac{x}{\bar{\nu}_+}}x^{-1}, & x > 0 \\ \lambda e^{-\frac{|x|}{\bar{\nu}_-}}|x|^{-1}, & x < 0 \end{cases},$$

with $\bar{\nu}_+ = \frac{\nu_+}{1-\varphi_2\nu_+}$, $\bar{\nu}_- = \frac{\nu_-}{1+\varphi_2\nu_-}$, and φ_2 given in Lemma 2 in Appendix.

[20] Again, for the derivation of the swaption price in the following proposition, we make use of the "freezing coefficients" technique.

Again, we note that not only can the term $\int_t^{T_j} \left(\sum_{k=j}^{j+N-1} \tilde{\omega}_k(t) \lambda(s, T_k) \right)^2 ds$ be calculated in closed form, but so can $\psi_J^{\mathbb{Q}_{j+1}^N}(u)$. Furthermore, a special case of the above valuation formula is obtained for the case $N = 1$. With $N = 1$, the swap rate is indeed equal to the three-month LIBOR rate. Since for $N = 1$ the term φ_2 vanishes, the pricing result in Proposition 6 corresponds to the one in Proposition 5 for caplets. Hence, in concluding this section, we can say that our flexible yet parsimonious time-changed Lévy model allows analytical pricing not only for caps but also for swaptions. Furthermore, the resulting formulae are consistent with each other.

5. Estimation

Implied volatilities for caps and swaptions are quoted under Black (1976)'s model, which assumes log-normally distributed forward LIBOR/swap rates. To convert the implied volatility quotes into the option prices used in the estimation, we need the zero-coupon bond prices (see also Appendix B for details). We obtain from Bloomberg the U.S. dollar forward LIBOR rates at maturities of one, two, three, six, nine, and 12 months and U.S. dollar swap rates with various maturities. Relying on the Nelson and Siegel (1987) parametric form, we bootstraped the forward three-month forward LIBOR rate curve.

The model uses two state variables, namely the activity rates V_t and ν_t, to capture the variation of the implied volatility surface in the caps and swaptions market over time. To estimate the model parameters, we cast the model into state space form by treating the state variables as hidden states. The implied volatility quotes from the caps and swaptions market serve as observations with errors. We employ a nonlinear filter, the unscented Kalman filter,[21] to extract the levels of the states at each date in our sample. The model parameters are estimated by maximizing the likelihood defined on the forecasting errors of option prices.

For the state space formulation, we treat the two activity rates as unobservable state variables. Hence, their dynamics will constitute the state propagation equations, which we formulate in discrete time as

$$[V_{t+1}, \nu_{t+1}]' = f(V_t, \nu_t; \Theta) + \sqrt{\Sigma}\varepsilon_{t+1},$$

[21] For a general treatment of unscented Kalman filters, see Wan and Van Der Merwe (2000) and Leippold and Wu (2007) for an application to term structure modeling.

where

$$f\left(V_t,\nu_t;\Theta\right) \quad = \quad \left(\begin{array}{c} \kappa_W\theta_W\Delta t+(1-\kappa_W^{\mathbb{P}}\Delta t)V_t^W \\ \kappa_J\theta_J\Delta t+(1-\kappa_J^{\mathbb{P}}\Delta t)\nu_t^J \end{array}\right), \qquad \Sigma_t=\left(\begin{array}{cc} \sigma_W^2V_t^W & 0 \\ 0 & \sigma_J^2\nu_t^J \end{array}\right)\Delta t,$$

with $\kappa_W^{\mathbb{P}}=\kappa_W-\sigma_W\gamma^V$ and $\kappa_J^{\mathbb{P}}=\kappa_J-\sigma_J\gamma^\nu$. We denote by $\Delta t=7/365$ the weekly frequency of the data we apply in the estimation. The term ε_{t+1} denotes an *iid* bivariate standard normal innovation. For the measurement equation, we write

$$y_t \quad = \quad h(V_t,\nu_t;\Theta)+\sqrt{\Omega}e_t,$$

where the vector y_t contains the observed market prices of Caps/Floors and Swaptions at time t scaled by their respective vega, i.e., their sensitivity to volatility changes. The function $h(\cdot)$ denotes the model-implied option prices as a function of our parameter set Θ and the state vector $[V_t,\nu_t]'$. To obtain cap/floor and swaption prices from the implied volatility quotes, we invert them by using the Black (1976) model. Appendix B presents the details on how we computed the option prices from the market data. For the pricing errors e_t, we assume independence and normal distribution with zero mean and constant diagonal covariance matrix Ω.

To estimate the model parameters, we define the quasi log-likelihood value for each week's observation on the option prices assuming that the forecasting errors are normally distributed:

$$l_{t+1}(\Theta)=-\frac{1}{2}\ln\left|\overline{A}_t\right|-\frac{1}{2}\left(\left(y_{t+1}-\overline{y}_{t+1}\right)^\top\left(\overline{A}_{t+1}\right)^{-1}\left(y_{t+1}-\overline{y}_{t+1}\right)\right), \tag{29}$$

where $\overline{y}$ denotes the model-implied option prices and $\overline{A}$ denotes the covariance on the model-implied option prices. We choose the model parameters to maximize the log-likelihood of the data series, which is a summation of the weekly log-likelihood values

$$\hat{\Theta}\equiv\arg\max_{\Theta}\mathcal{L}(\Theta,\{y_t\}_{t=1}^N), \quad \text{with} \quad \mathcal{L}(\Theta,\{y_t\}_{t=1}^N)=\sum_{t=0}^{N-1}l_{t+1}(\Theta), \tag{30}$$

where $N=158$ is the number of weeks in our sample, Θ denotes the parameter set to be estimated, and $\hat{\Theta}$ denotes the optimal parameters. Our full model specification has 15 parameters,

$$\Theta=\left\{\beta_1,\beta_2,\beta_3,\beta_4,\kappa_W,\theta_W,\sigma_W,\kappa_J,\theta_J,\sigma_J,\rho,\nu_+,\nu_-,\gamma^V,\gamma^\nu\right\},$$

which govern the dynamics of the underlying LIBOR forward rate and two state variables $\{V_t,\nu_t\}$ to price the time series and cross-sectional behavior of 161 interest rate options each week corresponding to a total of $25,438$ contracts.

Despite its richness in economic structures and flexibility in allowing separate sources of volatility variation, the model is very parsimonious in terms of the number of free parameters. In particular, its parsimony and the large number of option prices available allow us to identify the model parameters with strong statistical significance.

6. Results

In the following, we discuss our estimation results for the theoretical model developed in the previous sections.

6.1. Parameter estimates

Table 3 gives the parameter estimates together with their standard errors and the log-likelihood. As discussed in Section 2, we need a large and significantly negative correlation parameter ρ to fit the implied volatility skew in both the caps and swaptions market in our model. Indeed, we get $\rho = -0.844$. If we take the sample average of the activity rate V_t, our estimated value of ρ implies a correlation between innovations in the forward rate and its stochastic volatility of $\rho\sigma_W\overline{V_t} = -0.41$.

As for the jump parameters ν^+ and ν^-, we find that they are highly significant. Hence, during the financial crisis, jumps were an integral part of the forward rate dynamics, both in the LIBOR forward rates and in the forward swap rates. As the asymmetry between negative and positive jump sizes is small, we also estimated a restricted model with equal jump sizes. We find that, based on a likelihood ratio test, we can reject it in favor of the unrestricted model.

[Table 3 about here.]

Turning to the risk premium parameter γ^V on the stochastic activity rate V_t, we get a moderate value of -0.064 which, however, is statistically significant. In unreported results using caps data only for the estimation, we were not able to generate an estimate for γ^V different from zero. Hence, the inclusion of swaptions data clearly helps to identify the risk premium on stochastic volatility. Compared to the risk premium parameter γ^V, the parameter for the jump risk premium γ^ν is much larger. Combining the market price of risk coefficient estimates with the extracted

risk factors, we can compute the instantaneous risk premium on the two risk factors, i.e., $\sigma_W \gamma^V V_t$ for the instantaneous variance rate and $\sigma_J \gamma^\nu \nu_t$ for the jump activity rate. When we take sample averages for the activity rates, we get a mean risk premium value of -1% and -29%, respectively. Hence, both the magnitude and the time variation of the jump risk premium clearly dominate that of the variance risk premium.

Given the negative values for γ^V and γ^ν, the mean reversion speed parameters κ_W and κ_J are both smaller under the terminal forward measure $\mathbb{Q}_n$ than under the historical measure $\mathbb{P}$. Furthermore, the low $\mathbb{Q}_n$-values indicate a high persistence under the pricing measure. Under $\mathbb{P}$, the mean reversion speed of V_t still remains low ($\kappa_W^{\mathbb{P}} = 0.07$), given the low volatility risk premium. In contrast, for ν_t the mean reversion speed ($\kappa_J^{\mathbb{P}} = 1.97$) suggests a more transient jump activity rate under the historical measure. Finally, the estimated values β_i that specify the deterministic volatility function $\lambda(t,T)$ produce a downward sloping volatility curve with $\lim_{t\to T} \lambda(t,T) = 0.34$ and $\lim_{T\to\infty} \lambda(t,T) = 0.08$.

To gain intuition on the role of different parameters on the volatility surface, we shock some of the estimated parameters that are of particular interest, namely the correlation parameter ρ and the jump sizes ν_+ and ν_-, respectively. As we want to see the parameters' impact across the moneyness, option maturity, and swap tenor dimension, we focus only on the swaption cube. In Figure 5, the solid lines in each panel represent the implied volatilities of the swaption cube generated by our model with all parameters set equal to their estimated values and the activity rates set equal to their sample averages. For our analysis, we use swaption implied volatilities with an option maturity of one year and a swap tenor of five years.

We first analyze the impact of parameter shocks along the option maturity dimension. In Figure 5, Panels A and B display the responses of the swaption implied volatility to changes in ρ and $\nu_\pm$. In Panel A, the implied volatility decreases sharply with maturity when we set $\rho = 0$ (dashed line). For a larger (negative) correlation $\rho = -0.5$ (dash-dotted line), this decline is less dramatic. Hence, the correlation parameter may not only serve as a mechanism to generate negative skew, but also to generate persistency in the implied volatility along the option maturity dimension. Changes in the jump sizes $\nu_\pm$ have only a moderate effect on the implied volatilities as a function of option maturity. Increasing ν_+ to 0.05 and freezing ν_- at zero (dashed line), the term structure is slightly shifted downwards. When we freeze ν_+ at zero and let ν_- increase to 0.05 (dashed-dotted line), the effect is

even smaller. When we symmetrically increase the jump sizes to $\nu_{\pm} = 0.05$ (dashed line with dots as markers), the term structure across the option maturity dimension remains practically unchanged compared with our current estimates, which are also almost symmetrical, but much smaller (0.016 and 0.018, respectively). Hence, along the option maturity dimension, the asymmetry between positive and negative jumps has a larger effect than the absolute values of the jumps.

Next, we plot the same responses as above, but along the swap tenor dimension (Panels C and D, Figure 5). We see that a change in the correlation parameter ρ influences equally the implied volatilities at different swap tenors. Hence, changes in ρ lead to a parallel shift of the term structure and not to a shift in the steepness as in Panel A. Changes in the jump sizes $\nu_{\pm}$ have, to a lesser extent, the same effects. The impact is not as significant as in the case of ρ, but it is more pronounced than the effect along the option maturity dimension in Panel B. In Panel D, an asymmetrical shock to the jump sizes leads to a parallel downward shift, but when we symmetrically increase the jump sizes, the term structure exhibits a parallel upward shift. This behavior corresponds to our intuition. When we increase the negative jump parameter, future LIBOR rates tend to be lower. Through the channel of the leverage effect, lower rates will lead to higher volatilities. Similarly, when we increase ν_{+} the implicit volatility will be lower.

Finally, we plot the responses along the moneyness dimension (Panels E and F, Figure 5). For the correlation parameter, as expected, we cannot generate a negative skew with $\rho = 0$ (Panel E, dashed line). The implied volatility curve becomes flat. When correlation turns negative, we obtain a negative skew. While shocks in $\nu_{\pm}$ only have moderate impacts along the term structure dimensions, they do have a strong impact along the moneyness dimension (Panel F). When we increase ν_{-}, the implied volatility not only increases due to the link with the leverage effect, but also the implied volatility skew becomes more negative (dash-dotted line). On the other hand, when we increase only ν_{+}, volatility decreases while the skew becomes flatter (dashed line). When we symmetrically increase the jumps sizes, the skew moves in an almost parallel fashion. Hence, by splitting up the jumps sizes into negative and positive parts, we can fine-tune the level and steepness of the skew along the moneyness dimension.[22]

[22] We remark that we also estimated the model on a restricted data set, neglecting the information from non-ATM swaptions. We were not able to estimate the jump parameters with statistical significance. Hence, the crucial role of these parameters as an important model device further supports the inclusion of non-ATM swaption quotes into the estimation.

To summarize the above analysis, the parameter ρ is essential for all three dimensions of the swaption cube. Along the option maturity dimension, it governs the steepness of the term structure. Along the swap tenor dimension, it influences the level of the term structure and, finally, along the moneyness dimension it is essential to generate a negative skew. In contrast, the jump parameters $\nu_{\pm}$ do not play a significant role along the option maturity dimension. They play a moderate role in the swap tenor dimension. Furthermore, the steepness of the negative skew is driven by the magnitude of the negative shock ν_{-} relative to ν_{+}.

[Figure 5 about here.]

6.2. Pricing errors

In Tables 4 to 6 we present the root mean squared pricing errors (RMSE) and the mean pricing errors (MPE) on caps and swaptions implied volatilities, defined as the difference in percentage points between the model-implied values and the market-implied volatility quotes. Overall, we find that for intermediate and long maturities, our model performs remarkably well. The cap pricing errors in Table 4 indicate that the model's performance suffers mostly at the short end of option maturities, especially for the one year maturity. Short maturity contracts are underpriced by the model. However, the pricing performance considerably improves with increasing maturity. For longer maturities, there is a tendency to underprice out-of-the money and overprice in-the-money contracts.

[Table 4 about here.]

For the ATM swaptions implied volatilities in Table 5, we observe a similar pattern. The model struggles mostly for short option maturities and short swaption tenors, an observation that also holds true for the non-ATM swaptions in Table 6. However, across moneyness there is no clear pattern in terms of over- and underpricing as is the case for in-the-money and out-of-the-money caps.

[Tables 5 and 6 about here.]

The substantially higher pricing errors for the caps and swaptions market at shorter maturities call for further investigation. Ultimately, the caps and swaptions markets must be closely connected, as they both originate from derivatives written on the LIBOR forward rate. However, during periods of extreme market turmoil, the two markets might exhibit different behaviors due to differences in how the uncertainty regarding the intensified liquidity situation in the interbank market propagates through the caps and swaptions markets. Therefore, we next analyze the behavior of the pricing errors across time to see whether the caps and swaptions market become disintegrated or whether they suffer from the same deficiencies.

[Figure 6 about here.]

In Figure 6, we plot the time series of RMSE (Panel A) and the MPE (Panel B) for caps implied volatilities. We split the time series into long maturities and short maturities. For the first period of our data sample with the financial crisis already in full swing, the pricing errors in terms of RMSE remain remarkably low. In addition, until October 2008, we do not observe a bias in the model's pricing performance with the MPE close to zero. However, the pricing performance deteriorates considerably around April 2009 with substantial underpricing of short maturity contracts. This mispricing remains high until the end of our sample. Interestingly, this period of persistent mispricing of short maturity contracts coincides with the period of high implied volatilities at these maturities (see Figure 1). Hence, our model suffers when the volatility term structure is unusually steep.

For the swaptions implied volatilities, we observe a similar pattern. Swaptions have two maturity dimensions, the maturity of the swaption and the tenor of the swap. In Figure 7, Panels A and B, we first analyze the pricing errors along the swap tenor dimension. The errors start to increase at the same time as they do for the caps market. The underpricing of the swaptions on short tenor swaps exhibit substantial and systematic underpricing after April 2009, although to a lesser extent than in the caps market. In Figure 7, Panels D and C, we analyze the pricing errors across option maturities. There seems to be no systematic over- or underpricing. However, if we further split the data and plot the time series of short maturity swaptions with short swap tenors, the underpricing becomes again large and systematic (Panel D, dotted line). As we have shown in our theoretical derivations, the LIBOR rate is a special case of a swap rate with $N = 1$. Hence, it

is not surprising that the pricing performance of the model for swaptions with short swap tenors resembles the pricing performance of the caps implied volatilities. Indeed, when we calculate the correlation between the pricing errors of these two time series, we find a correlation of 84% for the RMSE and of 78% for the MPE. Hence, we may argue that both the pricing error and the pricing bias for caps and swaptions with short swap tenors may have a common cause. However, for mid- and longterm contracts, our model performs remarkably well over the whole sample period for both caps and swaptions.

[Figure 7 about here.]

A potential explanation for the model's deteriorating performance towards the end of the sample period might be that increased uncertainty materializes especially for short term contracts and dries out their liquidity. When we look at the figures, we could argue that the pricing performance of our model deteriorates first around fall 2008 and again in spring 2009. We could link the first deterioration with the LIBOR–OIS[23] spread. Although there was already a sharp rise in the term spreads on August 9, 2007, associated with market concerns related to subprime mortgage market, the spreads further skyrocketed from around 100 basis points to 350 basis points, following the announcement that Lehman Brothers had filed for Chapter 11 bankruptcy in September 2008.

The Lehman bankruptcy certainly had an adverse effect on the pricing performance of our (or any) model. Interestingly however, the pricing errors increase again in spring 2009, showing a strong persistency. They remain high until the end of our sample period. We conjecture that this systematic bias might be caused by a change in market practice. Indeed, as of the writing of this paper, financial market professionals are still coming to grips with the many changes that have occurred in pricing practices since the financial crisis. The basis between LIBOR and OIS, as well as between different parts of the LIBOR curve, blew out dramatically. This prompted some major changes in valuation methodologies. Far from using a single LIBOR curve to discount everything, many dealers started to develop multi-curve valuation models. Single curve and multi-curve approaches can diverge substantially in pricing and risk calculations. If the market indeed adopted a multi-curve approach on a large scale, then our single-curve model might generate a systematic pricing error. As research on multi-curve modeling is still evolving and there is currently

[23]OIS stands for "overnight indexed swap."

no common market practice,[24] a further substantiation of our conjecture is beyond the scope of this paper, yet it is an interesting research topic in its own right.

6.3. Dynamics of activity rates

In Figure 8, we plot the extracted state variables V_t and ν_t from the our estimation over the entire period, August 7, 2007 to August 11, 2010. In Panel A, we plot the activity rate V_t. We observe that in 2008 there was a constant increase in this rate with a consolidation at a high level after early 2009. When we look at the jump activity rate ν_t in Panel B, we see a dramatic increase during the second half of 2009 not only in its level, but also in its variation. To provide some intuition about the dynamic behavior of the two state variables V_t and ν_t and their different roles during the financial market crisis, we split our sample into three episodes linked to specific market events.

[Figure 8 about here.]

The first episode is characterized by an increasing volatility V_t and started in the fall of 2007, when the interbank funding market experienced liquidity problems, as indicated by the increasing LIBOR–OIS spread,[25] which reached 108 basis points on December 6, 2007. At that time, the investment bank Lehman Brothers reported large write downs and subsequently, on March 17, 2008, Bear Stearns collapsed. These events are clearly captured by the first spikes in the activity rates, particularly by the activity rate V_t driving the stochastic volatility of LIBOR rates. This period was followed by another wave of events in the fall of 2008 which triggered a further increase in the activity rate V_t. On September 7, 2008, the government-sponsored entities Fannie Mae and Freddie Mac were placed into conservatorship by the U.S. government. Fannie Mae and Freddie Mac, two key players in the caps and swaptions markets, had large hedges related to their engagement in the mortgage backed securities market. On September 15, 2008, Lehman Brothers filed for bankruptcy, which undoubtedly spurred increasing uncertainty in the interbank market. During this period, not only the activity rate V_t, but also ν_t, increased substantially.

[24] See, e.g., Bianchetti and Carlicchi (2011) among others.

[25] During the financial crisis, the LIBOR–OIS (overnight indexed swap rate) spread was considered a key indicator for the degree of liquidity in the interbank market.

The second episode starts at the end of 2008. On November 25, 2008, the Fed announced its first quantitative easing program (QE1) to buy $500 billion in mortgage bonds with effect from January, 2009.[26] Even though no MBS had yet been purchased by the Fed, the mere announcement of the QE1 program led to an immediate reduction in the level of the stochastic volatility V_t. Hence, the Fed signaled strong and credible backing for mortgage markets in particular and for interest rate markets in general.[27] Subsequently, on January 5, 2009, the Federal Reserve began purchasing fixed-rate mortgage backed securities guaranteed by Fannie Mae and Freddie Mac, which further stabilized the volatility in the caps and swaptions markets. However, the average level of ν_t remained high, which might reflect the market's general unease with the uncertainty surrounding the impact of the Fed's intervention. Then, on May 7, 2009, the results from the U.S. Federal stress test of the largest 19 U.S. bank holding companies were announced. The stress test revealed that the 19 companies could potentially lose $600 billion during 2009 and 2010 if the economy were to follow the adverse scenario considered in the stress test. Subsequently, on May 8 and May 12, respectively, Fannie Mae and Freddie Mac announced large write downs. These events seem to have triggered another period of increasing uncertainty, which hindered V_t from decline further to mid-2008 levels and increased the level of ν_t to new heights. Hence, market participants may have expected some sudden dramatic changes in future interest rates.

The third and final episode starts towards the end of 2009 and beginning of 2010. On March 31, 2010, the Federal Reserves' mortgage bond buying program ended. The 30 year fixed rates rose to 5.125%. This increase was caused by investors exiting mortgage bond trades before the Fed money was gone. The uncertainty surrounding the end of QE1 caused a large variation in ν_t. This variation was further nourished by the debt problems in Greece. On May 9, 2010, the International Monetary Fund (IMF) decided to provide financial support to Greece. The increased awareness of a potentially contagious sovereign debt crisis in Europe further increased uncertainty in the interest rate markets and drove global investors into U.S. mortgage and Treasury bonds. Subsequently, the 30 year fixed rate dropped to 4.78%. However, the uncertainty about the future course of interest rates is reflected by the substantial variation in the stochastic arrival rate for

[26]The goal of the QE1 program, as stated by the Federal Reserve in their press release on November 25, 2008, was to "...reduce the cost and increase the availability of credit for the purchase of houses, which in turn should support housing markets and foster improved conditions in financial markets more generally." See, http://www.federalreserve.gov/newsevents/press/monetary/20081125b.htm.

[27]The study by Hancock and Passmore (2011) is in line with our argumentation. They show that the Fed's announcement reduced mortgage rates by about 85 basis points between November 25 and December 31, 2008.

jumps ν_t in the LIBOR rates during the end of our sample period.

7. Conclusion

We introduced a novel time-changed Lévy LIBOR market model. Its design was motivated by a preliminary analysis of the stylized facts about the implied volatilities of the cap surface and the swaption cube. Our model is analytically tractable and yet flexible enough to price caps and swaptions simultaneously. The parsimonious model structure facilitates the identification and stability of the parameter estimates, which is crucial for risk management and hedging.

We found that the incorporation of a jump component and a stochastic volatility factor that is highly correlated with changes in interest rates is crucial for the simultaneous pricing of caps and swaptions. Especially for intermediate and long maturities, we found evidence that the markets for caps and swaptions have been well integrated even during the financial crisis. To explain the volatility skew, we could also have extended the model with a CEV-type structure. However, such an extension is beyond the scope of our paper. Nevertheless, it could be an interesting avenue for future research.

The analysis of the pricing errors during the recent financial crisis reveals interesting avenues for future research. In particular, it would be interesting to see what drives the pricing errors of short maturity contracts especially since early 2009. Hence, depending on the availability of data, an important direction for future research based on our results would be the development of models that include additional drivers, such as liquidity or sovereign credit risk and the potential impact of changing market practices, such as the introduction of multiple discounting curves.

References

Babbs, S. H., Webber, N., 1997. Term structure modelling under alternative official regimes; in Mathematics of derivatives securities eds. M.A.H. Dempster and S.R. Pliska. Cambridge University Press, Cambridge United Kingdom.

Bianchetti, M., Carlicchi, M., 2011. Interest rates after the credit crunch: Multiple curve vanilla derivatives and SABR. Capco Journal of Financial Transformation 32.

Bjork, T., 2004. Arbitrage theory in continuous time. Oxford University Press.

Bjork, T., Kabanov, Y., Runggaldier, W., 2002. Bond market structure in the presence of marked point processes. Mathematical Finance 7, 211–239.

Black, F., 1976. The pricing of commodity contracts. Journal of Financial Economics 3, 167–179.

Brigo, D., Mercurio, F., 2002. On the joint calibration of the LIBOR market model to caps and swaptions market volatilities. RISK pp. 117–121.

Brigo, D., Mercurio, F., 2006. Interest rate models: Theory and practice. Springer Finance.

Carr, P., Madan, D. B., 1999. Option valuation using the Fast Fourier Transform. Journal of Computational Finance 2, 61–73.

Carr, P., Wu, L., 2004. Time-changed Lévy processes and option pricing. Journal of Financial Economics 71, 113–141.

Carr, P., Wu, L., 2007. Stochastic skew in currency options. Journal of Financial Economics 86, 213–247.

Carr, P., Wu, L., 2008. Leverage effect, volatility feedback, and self-exciting market disruptions: Disentangling the multi-dimensional variations in S&P500 Index Options. Working Paper.

Casassus, J., Collin-Dufresne, P., Goldstein, B., 2005. Unspanned stochastic volatility and fixed income derivatives pricing. Journal of Banking and Finance 29, 2723–2749.

Cont, R., Tankov, P., 2004. Financial modelling with jump processes. Chapman and Hall/CRC, Financial Mathematics Series.

Das, S. R., 2002. The surprise element: Jumps in interest rates. Journal of Econometrics, Vol. 106, pp. 27-65, 2002.

Driessen, J., Klaassen, P., Melenberg, B., 2003. The performance of multi-factor term structure models for pricing and hedging caps and swaptions. Journal of Financial and Quantitative Analysis 38, 635–672.

Duarte, J., 2008. The causal effect of mortgage refinancing on interest rate volatility: Empirical evidence and theoretical implications. Review of Financial Studies 21, 1689–1731.

Eberlein, E., Kluge, W., 2006. Exact pricing formulae for caps and swaptions in a Lévy term structure model. Journal of Computational Finance 9, 99–125.

Eberlein, E., Liinev, J., 2007. The Lévy swap market model. Applied Mathematical Finance 14, 171–196.

Eberlein, E., Ozkan, F., 2005. The Lévy LIBOR model. Finance and Stochastics 9, 327–348.

Eberlein, E., Raible, S., 1999. Term structure models driven by general Lévy Processes. Mathematical Finance 9, 31–54.

El-Jahel, L., Lindberg, H., Perraudin, W., 1997. Interest rate distributions, yield curve modelling and monetary policy; in Mathematics of derivatives securities eds. M.A.H. Dempster and S.R. Pliska. Cambridge University Press, Cambridge United Kingdom.

Fan, R., Gupta, A., Ritchken, P., 2003. Hedging in the possible presence of unspanned stochastic volatility: Evidence from swaption markets. Journal of Finance 58, 2219–2248.

Galluccio, S., Ly, J.-M., Scaillet, O., Huang, Z., 2007. Theory and calibration of swap market models. Mathematical Finance 17, 111–141.

Hancock, D., Passmore, W., 2011. Did the federal reserves MBS purchase program lower mortgage rates?. Working paper. Finance and Economics Discussion Series (FEDS), Divisions of Research & Statistics and Monetary Affairs Federal Reserve Board, Washington, D.C.

Heidari, M., Wu, L., 2003. Are interest rate derivatives spanned by the term sturcture of interest rates?. Journal of Fixed Income 13, 75–86.

Jagannathan, R., Kaplin, A., Sun, S. G., 2003. An evaluation of multi-factor CIR models using LIBOR swap rates and cap and swaption prices. Journal of Econometrics 116, 113–146.

Jarrow, R., Li, H., Zhao, F., 2007. Interest rate caps "smile" too! But can the LIBOR market models capture the smile?. Journal of Finance 62, 345–382.

Johannes, M., 2004. The statistical and economic role of jumps in continuous-time interest rate models. Journal of Finance 59, 227–260.

Kluge, W., 2005. Time-inhomogenous Lévy processes in interest rate and credit risk models. PhD Thesis, University of Freiburg.

Leippold, M., Wu, L., 2007. Design and estimation of multi-currency quadratic models. Review of Finance 11, 167–207.

Li, H., Zhao, F., 2009. Nonparametric estimation of state-price densities implicit in interest rate cap prices. Review of Financial Studies 22, 4335–4376.

Longstaff, F. A., Santa-Clara, P., Schwartz, E. S., 2001. The relative valuation of caps and swaptions: Theory and empirical evidence. Journal of Finance 56, 2067–2109.

Merton, R. C., 1976. Option pricing when underlying stock returns are discontinuous. Journal of Financial Economics 3, 125–144.

Musiela, M., Rutkowski, M., 2005. Martingale methods in finance. Springer, New York.

Nelson, C. R., Siegel, A. F., 1987. Parsimonious modeling of yield curves. Journal of Business 60, 473–489.

Rebonato, R., McKay, K., White, R., 2009. The SABR/LIBOR market model. John Wiley and Son.

Trolle, A. B., Schwartz, E. S., 2012. The swaption cube. Working paper. .

Wan, E., Van Der Merwe, R., 2000. The unscented kalman filter for nonlinear estimation. In: Adaptive Systems for Signal Processing, Communications, and Control Symposium 2000. AS-SPCC. The IEEE 2000 pp. 153 –158.

Wu, L., 2008. Modelling financial security returns using Lévy processes. Handbooks in operations research and management science: Financial Engineering 15.

Appendix A

Proof of Proposition 1

From the specification given in equations (4)–(5), we can apply Ito's formula for Lévy processes (e.g., Cont and Tankov (2004)) to obtain the dynamics of the forward LIBOR rate $L(t,T_j)$ under the T_{j+1}-forward measure as follows,

$$\begin{aligned}\frac{dL(t,T_j)}{L(t,T_j)} &= b(t,T_j,T_{j+1})dt + \frac{1}{2}\lambda^2(t,T_j)dt + \frac{1}{2}V_t^W dt \\ &+ \int_{-\infty}^{0}(e^x-1-x)\,\pi_{J^-}^{\mathbb{Q}_{j+1}}(dx)\nu_t^J dt + \int_0^{\infty}(e^x-1-x)\,\pi_{J^+}^{\mathbb{Q}_{j+1}}(dx)\nu_t^J dt \\ &+ \lambda(t,T_j)dB_t^{Q_{j+1}} + \sqrt{V_t^W}dW_t^{Q_{j+1}} + \int_{-\infty}^{0}(e^x-1)\left(\mu^-(dt,dx) - \pi_{J^-}^{Q_{j+1}}(x)dx\nu_t^J dt\right) \\ &+ \int_0^{\infty}(e^x-1)\left(\mu^+(dt,dx) - \pi_{J^+}^{Q_{j+1}}(x)dx\nu_t^J dt\right).\end{aligned}$$

To ensure that $L(t,T_j)$ is a martingale under the T_{j+1}-forward measure, the drift must equal zero, which gives the drift condition in the proposition. ■

Proof of Proposition 2

The proposition follows by (backward) induction starting from the dynamics of the forward LIBOR rate under the terminal forward measure $\mathbb{Q}_n$. Consider first the change of measure from $\mathbb{Q}_n$ to $\mathbb{Q}_{n-1}$. The Radon–Nikodym derivative for changing the measure from the T_n-forward measure, $\mathbb{Q}_n$, to the T_{n-1}-forward measure, $\mathbb{Q}_{n-1}$, is

$$\frac{d\mathbb{Q}_{n-1}}{d\mathbb{Q}_n}_{|\mathcal{F}_t} = \frac{P(t,T_{n-1})/P(0,T_{n-1})}{P(t,T_n)/P(0,T_n)}. \tag{A.1}$$

Recall that the forward LIBOR rates $L(t,T_{n-1})$ are defined at time t by

$$L(t,T_{n-1}) = \frac{1}{T_n - T_{n-1}}\left(\frac{P(t,T_{n-1})}{P(t,T_n)} - 1\right), \tag{A.2}$$

where T_n denotes the terminal maturity in the LIBOR tenor structure. This can be rewritten for $T_n - T_{n-1} = \delta$ as

$$\frac{P(t,T_{n-1})}{P(t,T_n)} = \delta L(t,T_{n-1}) + 1, \tag{A.3}$$

where $\frac{P(t,T_{n-1})}{P(t,T_n)}$ can be viewed as a forward price process. Consider now the dynamics of this forward price process:

$$\begin{aligned} d\left(\frac{P(t,T_{n-1})}{P(t,T_n)}\right) &= \delta L(t,T_{n-1})\left(\lambda(t,T_{n-1})dB_t^{\mathbb{Q}_n} + \sqrt{V_t^W}dW_t^{\mathbb{Q}_n}\right. \\ &\quad + \int_{-\infty}^{0}(e^x-1)\left(\mu^-(dt,dx) - \pi_{J^-}^{\mathbb{Q}_n}(x)dx\nu_t^J dt\right) \\ &\quad \left. + \int_0^{\infty}(e^x-1)\left(\mu^+(dt,dx) - \pi_{J^+}^{\mathbb{Q}_n}(x)dx\nu_t^J dt\right)\right) \\ &= \left(\frac{P(t,T_{n-1})}{P(t,T_n)}\right)\left(\gamma_\lambda(t,T_{n-1},T_n)dB_t^{\mathbb{Q}_n} + \gamma_V(t,T_{n-1},T_n)dW_t^{\mathbb{Q}_n}\right. \\ &\quad + \int_{-\infty}^{0}\gamma_J(t,T_{n-1},T_n)\left(\mu^-(dt,dx) - \pi_{J^-}^{\mathbb{Q}_n}(x)dx\nu_t^J dt\right) \\ &\quad \left. + \int_0^{\infty}\gamma_J(t,T_{n-1},T_n)\left(\mu^+(dt,dx) - \pi_{J^+}^{\mathbb{Q}_n}(x)dx\nu_t^J dt\right)\right) \end{aligned}$$

using the fact that $L(t,T_{n-1})$ is a martingale under the measure $\mathbb{Q}_n$, and that

$$\begin{aligned} \gamma_\lambda(t,T_{n-1},T_n) &= \frac{\delta L(t,T_{n-1})}{\delta L(t,T_{n-1})+1}\lambda(t,T_{n-1}) \\ \gamma_V(t,T_{n-1},T_n) &= \frac{\delta L(t,T_{n-1})}{\delta L(t,T_{n-1})+1}\sqrt{V_t^W} \\ \gamma_J(t,T_{n-1},T_n) &= \frac{\delta L(t,T_{n-1})}{\delta L(t,T_{n-1})+1}(e^x-1). \end{aligned}$$

Simplifying the above by putting $F_B(t,T_{n-1},T_n) = \frac{P(t,T_{n-1})}{P(t,T_n)}$, and

$$\begin{aligned} H(t,T_n) &= \int_0^t \gamma_\lambda(s,T_{n-1},T_n)dB_s^{\mathbb{Q}_n} + \gamma_V(s,T_{n-1},T_n)dW_s^{\mathbb{Q}_n} \\ &+ \int_0^t\int_{-\infty}^{0}\gamma_J(t,T_{n-1},T_n)\left(\mu^-(dt,dx) - \pi_{J^-}^{\mathbb{Q}_n}(x)dx\nu_t^J dt\right) \\ &+ \int_0^t\int_0^{\infty}\gamma_J(t,T_{n-1},T_n)\left(\mu^+(dt,dx) - \pi_{J^+}^{\mathbb{Q}_n}(x)dx\nu_t^J dt\right), \end{aligned}$$

the stochastic differential equation can be reformulated as

$$dF_B(t,T_{n-1},T_n) = F_B(t,T_{n-1},T_n)dH(t,T_n) \tag{A.4}$$

from which we know the solution is the Doléans–Dade stochastic exponential given by[28]

$$F_B(t,T_{n-1},T_n) = F_B(0,T_{n-1},T_n)\mathcal{E}\left(H(t,T_n)\right). \tag{A.5}$$

[28]The term T_n in $H(t,T_n)$ indicates that the stochastic exponential is taken under the T_{n-1}-forward measure.

Therefore,

$$\frac{P(t,T_{n-1})/P(0,T_{n-1})}{P(t,T_n)/P(0,T_n)} = \mathcal{E}\left(H(t,T_n)\right). \tag{A.6}$$

We observe that the likelihood process we are looking for in order to change measures from the T_n-forward measure, $\mathbb{Q}_n$, to the T_{n-1}-forward measure, $\mathbb{Q}_{n-1}$, is defined by the stochastic exponential of the process $H(t,T_n)$ (which by definition is a $\mathbb{Q}_n$-martingale due to the martingale preserving property, see Proposition 8.23 in Cont and Tankov (2004)). Writing the measure transformation in more familiar terms,

$$\begin{aligned}
\frac{d\mathbb{Q}_{n-1}}{d\mathbb{Q}_n}_{|\mathcal{F}_t} &= \mathcal{E}\left(\int_0^t \gamma_\lambda(s,T_{n-1},T_n)dB_s^{\mathbb{Q}_n} + \gamma_V(s,T_{n-1},T_n)dW_s^{\mathbb{Q}_n}\right. && \text{(A.7)}\\
&+ \int_0^t\int_{-\infty}^0 \gamma_J(t,T_{n-1},T_n)\left(\mu^-(dt,dx) - \pi_{J^-}^{\mathbb{Q}_n}(x)dx\nu_t^J dt\right) && \text{(A.8)}\\
&+ \left.\int_0^t\int_0^\infty \gamma_J(t,T_{n-1},T_n)\left(\mu^+(dt,dx) - \pi_{J^+}^{\mathbb{Q}_n}(x)dx\nu_t^J dt\right)\right), && \text{(A.9)}
\end{aligned}$$

for all $t \in [0,T_{n-1}]$. We can now identify the Girsanov kernel in the measure transformation related to the Brownian motion part which allows us to change from one forward measure to another:

$$\begin{aligned}
dB_t^{\mathbb{Q}_{n-1}} &= dB_t^{\mathbb{Q}_n} - \langle dB_t^{\mathbb{Q}_n}, \gamma_\lambda(t,T_{n-1},T_n)dB_t^{\mathbb{Q}_n}\rangle = dB_t^{\mathbb{Q}_n} - \gamma_\lambda(t,T_{n-1},T_n)dt && \text{(A.10)}\\
dW_t^{\mathbb{Q}_{n-1}} &= dW_t^{\mathbb{Q}_n} - \langle dW_t^{\mathbb{Q}_n}, \gamma_V(t,T_{n-1},T_n)dW_t^{\mathbb{Q}_n}\rangle = dW_t^{\mathbb{Q}_n} - \gamma_V(t,T_{n-1},T_n)dt, && \text{(A.11)}
\end{aligned}$$

where $\langle\cdot,\cdot\rangle$ denotes the covariance. Moreover, we observe that the change of intensity of the jump component (e.g., Bjork, Kabanov, and Runggaldier (2002)) takes the form

$$\pi_J^{\mathbb{Q}_{n-1}}\nu^J = \left(1+\gamma_J(t,T_{n-1},T_n)\right)\pi_J^{\mathbb{Q}_n}\nu^J, \tag{A.12}$$

for $J = \{J^-, J^+\}$. Consider next the measure change $\mathbb{Q}_{n-1}$ to $\mathbb{Q}_{n-2}$. The Radon–Nikodym derivative for changing the measure from the T_{n-1}-forward measure, $\mathbb{Q}_{n-1}$, to the T_{n-2}-forward measure, $\mathbb{Q}_{n-2}$, is

$$\frac{d\mathbb{Q}_{n-2}}{d\mathbb{Q}_{n-1}}_{|\mathcal{F}_t} = \frac{P(t,T_{n-2})/P(0,T_{n-2})}{P(t,T_{n-1})/P(0,T_{n-1})}. \tag{A.13}$$

The dynamics of the forward price process is given by

$$\begin{aligned} d\left(\frac{P(t,T_{n-2})}{P(t,T_{n-1})}\right) &= \left(\frac{P(t,T_{n-2})}{P(t,T_{n-1})}\right)\Big(\gamma_\lambda(t,T_{n-2},T_{n-1})dB_t^{\mathbb{Q}_{n-1}} + \gamma_V(t,T_{n-2},T_{n-1})dW_t^{\mathbb{Q}_{n-1}} \\ &+ \int_{-\infty}^{0}\gamma_J(t,T_{n-2},T_{n-1})\left(\mu^-(dt,dx) - \pi_{J^-}^{\mathbb{Q}_{n-1}}(x)dx\nu_t^J dt\right) + \\ &\int_0^{\infty}\gamma_J(t,T_{n-2},T_{n-1})\left(\mu^+(dt,dx) - \pi_{J^+}^{\mathbb{Q}_{n-1}}(x)dx\nu_t^J dt\right)\Big), \end{aligned}$$

where

$$\begin{aligned} \gamma_\lambda(t,T_{n-2},T_{n-1}) &= \frac{\delta L(t,T_{n-2})}{\delta L(t,T_{n-2})+1}\lambda(t,T_{n-2}) \\ \gamma_V(t,T_{n-2},T_{n-1}) &= \frac{\delta L(t,T_{n-2})}{\delta L(t,T_{n-2})+1}\sqrt{V_t^W} \\ \gamma_J(t,T_{n-2},T_{n-1}) &= \frac{\delta L(t,T_{n-2})}{\delta L(t,T_{n-2})+1}\left(e^x-1\right). \end{aligned}$$

Similarly to the above, we end up with

$$\frac{P(t,T_{n-2})/P(0,T_{n-2})}{P(t,T_{n-1})/P(0,T_{n-1})} = \mathcal{E}\left(H(t,T_{n-1})\right), \tag{A.14}$$

where

$$\begin{aligned} H(t,T_{n-1}) &= \int_0^t \gamma_\lambda(s,T_{n-2},T_{n-1})dB_s^{\mathbb{Q}_{n-1}} + \gamma_V(s,T_{n-2},T_{n-1})dW_s^{\mathbb{Q}_{n-1}} \\ &+ \int_0^t\int_{-\infty}^0 \gamma_J(t,T_{n-2},T_{n-1})\left(\mu^-(dt,dx) - \pi_{J^-}^{\mathbb{Q}_{n-1}}(x)dx\nu_t^J dt\right) \\ &+ \int_0^t\int_0^{\infty} \gamma_J(t,T_{n-2},T_{n-1})\left(\mu^+(dt,dx) - \pi_{J^+}^{\mathbb{Q}_{n-1}}(x)dx\nu_t^J dt\right), \end{aligned}$$

and again we observe that the likelihood process we are looking for in order to change measures from the T_{n-1}-forward measure, $\mathbb{Q}_{n-1}$, to the T_{n-2}-forward measure, $\mathbb{Q}_{n-2}$, which is defined by the stochastic exponential of the process $H(t,T_{n-1})$, which by definition is a $\mathbb{Q}_{n-1}$-martingale. As above, we can write the measure transformation in more familiar terms as

$$\begin{aligned} \frac{d\mathbb{Q}_{n-2}}{d\mathbb{Q}_{n-1}{}_{|\mathcal{F}_t}} &= \mathcal{E}\left(\int_0^t \gamma_\lambda(s,T_{n-2},T_{n-1})dB_s^{\mathbb{Q}_{n-1}} + \gamma_V(s,T_{n-2},T_{n-1})dW_s^{\mathbb{Q}_{n-1}}\right. && \text{(A.15)} \\ &+ \int_0^t\int_{-\infty}^0 \gamma_J(t,T_{n-2},T_{n-1})\left(\mu^-(dt,dx) - \pi_{J^-}^{\mathbb{Q}_{n-1}}(x)dx\nu_t^J dt\right) && \text{(A.16)} \\ &+ \left.\int_0^t\int_0^{\infty} \gamma_J(t,T_{n-2},T_{n-1})\left(\mu^+(dt,dx) - \pi_{J^+}^{\mathbb{Q}_{n-1}}(x)dx\nu_t^J dt\right)\right), && \text{(A.17)} \end{aligned}$$

for all $t \in [0, T_{n-2}]$. We can now identify the Girsanov kernel in the measure transformation related to the Brownian motion part which allows us to change from one forward measure to another:

$$\begin{aligned} dB_t^{\mathbb{Q}_{n-2}} &= dW_{1,t}^{\mathbb{Q}_{n-1}} - \langle dB_t^{\mathbb{Q}_{n-1}}, \gamma_\lambda(t, T_{n-2}, T_{n-1}) dB_t^{\mathbb{Q}_{n-1}} \rangle = dB_t^{\mathbb{Q}_{n-1}} - \gamma_\lambda(t, T_{n-2}, T_{n-1}) dt \\ &= dB_t^{\mathbb{Q}_n} - \sum_{k=1}^{2} \gamma_\lambda \left(t, T_{n-k}, T_{n+1-k}\right) dt \qquad \text{(A.18)} \\ dW_t^{\mathbb{Q}_{n-2}} &= dW_t^{\mathbb{Q}_{n-1}} - \langle dW_t^{\mathbb{Q}_{n-1}}, \gamma_V(t, T_{n-2}, T_{n-1}) dW_t^{\mathbb{Q}_{n-1}} \rangle = dW_t^{\mathbb{Q}_{n-1}} - \gamma_V(t, T_{n-2}, T_{n-1}) dt \\ &= dW_t^{\mathbb{Q}_n} - \sum_{k=1}^{2} \gamma_V \left(t, T_{n-k}, T_{n+1-k}\right) dt. \qquad \text{(A.19)} \end{aligned}$$

The change of intensity of the jump component takes the form

$$\begin{aligned} \pi_J^{\mathbb{Q}_{n-2}} \nu^J &= \left(1 + \gamma_J(t, T_{n-2}, T_{n-1})\right) \pi_J^{\mathbb{Q}_{n-1}} \nu^J \qquad \text{(A.20)} \\ &= \prod_{k=1}^{2} \left(1 + \gamma_J(t, T_{n-k}, T_{n+1-k})\right) \pi_J^{\mathbb{Q}_n} \nu^J \qquad \text{(A.21)} \end{aligned}$$

for $J = \{J^-, J^+\}$. Continuing the same procedure along the entire tenor structure, we can, for $j = 2, \ldots, n$, summarize the forward measure transformations that define the family of spanning forward LIBOR rates related to the terminal measure (i.e., the $\mathbb{Q}_n$ measure):

$$\begin{aligned} dB_t^{\mathbb{Q}_{j-1}} &= dB_t^{\mathbb{Q}_n} - \sum_{k=1}^{n+1-j} \gamma_\lambda \left(t, T_{n-k}, T_{n+1-k}\right) dt \qquad \text{(A.22)} \\ dW_t^{\mathbb{Q}_{j-1}} &= dW_t^{\mathbb{Q}_n} - \sum_{k=1}^{n+1-j} \gamma_V \left(t, T_{n-k}, T_{n+1-k}\right) dt \qquad \text{(A.23)} \\ \pi_J^{\mathbb{Q}_{j-1}} \nu_t^J &= \prod_{k=1}^{n+1-j} \left(1 + \gamma_J(t, T_{n-k}, T_{n+1-k})\right) \pi_J^{\mathbb{Q}_n} \nu^J, \qquad \text{(A.24)} \end{aligned}$$

where

$$\begin{aligned} \gamma_\lambda(t, T_{n-k}, T_{n+1-k}) &= \frac{\delta L(t, T_{n-k})}{\delta L(t, T_{n-k}) + 1} \lambda(t, T_{n-k}) \\ \gamma_V(t, T_{n-k}, T_{n+1-k}) &= \frac{\delta L(t, T_{n-k})}{\delta L(t, T_{n-k}) + 1} \sqrt{V_t^W} \\ \gamma_J(t, T_{n-k}, T_{n+1-k}) &= \frac{\delta L(t, T_{n-k})}{\delta L(t, T_{n-k}) + 1} \left(e^x - 1\right), \end{aligned}$$

for the jump components, where $J = \{J^-, J^+\}$, respectively, as given in the proposition. ■

Proof of Proposition 3

We can proceed similarly to Proposition 2. Consider first $\mathbb{Q}_n$ to $\mathbb{Q}_{n-1}$:

$$\begin{aligned} d\widetilde{W}^{\mathbb{Q}_{n-1}} &= d\widetilde{W}^{\mathbb{Q}_n} - \langle d\widetilde{W}^{\mathbb{Q}_n}, \gamma_W(t, T_{n-1}, T_n)\sqrt{V_t^W}dW^{\mathbb{Q}_n}\rangle \\ &= d\widetilde{W}^{\mathbb{Q}_n} - \frac{\delta L(t, T_{n-1})}{\delta L(t, T_{n-1}) + 1}\sqrt{V_t^W}\rho dt. \end{aligned}$$

Now consider $\mathbb{Q}_{n-1}$ to $\mathbb{Q}_{n-2}$:

$$\begin{aligned} d\widetilde{W}^{\mathbb{Q}_{n-2}} &= d\widetilde{W}^{\mathbb{Q}_{n-1}} - \langle d\widetilde{W}^{\mathbb{Q}_{n-1}}, \gamma_W(t, T_{n-2}, T_{n-1})\sqrt{V_t^W}dW^{\mathbb{Q}_{n-1}}\rangle \\ &= d\widetilde{W}^{\mathbb{Q}_{n-1}} - \frac{\delta L(t, T_{n-2})}{\delta L(t, T_{n-2}) + 1}\sqrt{V_t^W}\rho dt, \end{aligned}$$

which can be related to the terminal measure, $\mathbb{Q}_n$:

$$d\widetilde{W}^{\mathbb{Q}_{n-2}} = d\widetilde{W}^{\mathbb{Q}_n} - \sum_{k=1}^{2} \frac{\delta L(t, T_{n-k})}{\delta L(t, T_{n-k}) + 1}\sqrt{V_t^W}\rho dt. \tag{A.25}$$

Continuing the same procedure along the entire tenor structure, we can, for $j = 2, \ldots, n$, summarize the forward measure transformations that define the family of measure changes for the stochastic volatility process by their relation to the terminal forward measure, $\mathbb{Q}_n$, as stated in the proposition. ■

Proof of Proposition 4

To prove Proposition 4, we need the following lemma.

Lemma 1. *The co-sliding forward swap rate can be approximated by*

$$R_j^N(t) \approx R_j^N(0) \exp\left(\int_0^t \sum_{k=j}^{j+N-1} \tilde{\omega}_k(0) dX_s + \textit{drift}\right), \tag{A.26}$$

where X_s is the Lévy process under the terminal forward LIBOR measure in (5) *and* $\tilde{\omega}_k(0) = \frac{\omega_k(0)L(0,T_k)}{R_j^N(0)}$ *with* $\omega_k(0) = \frac{P(0,T_{k+1})}{\sum_{k=j+1}^{j+N} P(0,T_k)}$.

Proof: We can represent the co-sliding forward swap rate as a weighted average of spanning forward LIBOR rates:

$$R_j^N(t) = \frac{P(t, T_j) - P(t, T_{j+N})}{\delta \sum_{k=j+1}^{j+N} P(t, T_k)} = \sum_{k=j}^{j+N-1} \omega_k(t) L(t, T_k) \tag{A.27}$$

where the weights are given by $\omega_k(t) = \frac{P(t,T_{k+1})}{\sum_{k=j+1}^{j+N} P(t,T_k)}$. To obtain analytical tractability, we freeze the weights $\omega_k(t)$ at time $t = 0$ and we use the approximation $ye^x \approx y + yx$ for x small.[29] Then,

$$\begin{aligned}
R_j^N(t) &\approx \sum_{k=j}^{j+N-1} \omega_k(0)L(t,T_k) = \sum_{k=j}^{j+N-1} \omega_k(0)L(0,T_k)\exp\left(\int_0^t dX_s + \text{drift}\right) \\
&\approx \sum_{k=j}^{j+N-1} \omega_k(0)L(0,T_k) + \sum_{k=j}^{j+N-1} \omega_k(0)L(0,T_k)\left(\int_0^t dX_s + \text{drift}\right) \\
&= R_j^N(0) + R_j^N(0)\left(\int_0^t \sum_{k=j}^{j+N-1} \frac{\omega_k(0)L(0,T_k)}{R_j^N(0)} dX_s + \text{drift}\right) \\
&\approx R_j^N(0)\exp\left(\int_0^t \sum_{k=j}^{j+N-1} \tilde{\omega}_k(0) dX_s + \text{drift}\right),
\end{aligned}$$

where $X_t^{\mathbb{Q}_n}$ is the Lévy process under the terminal forward measure given in (5) and $\tilde{\omega}_k(0) = \frac{\omega_k(0)L(0,T_k)}{R_j^N(0)}$. □

The above lemma allows us to approximately model the co-sliding forward swap rate as an exponential of the Lévy process X_s under the terminal forward LIBOR measure. However, for pricing purposes, it is convenient to formulate the forward swap rate dynamics under the appropriate terminal co-sliding forward swap measures under which the forward swap rate is a martingale. By doing so, we will be consistent with the Black (1976) model, which is currently market practice for valuing swaption derivatives.

Similar to the LMM, we can construct an entire family of co-sliding forward swap rates by backward induction starting from the terminal co-sliding forward swap measure for a given N. However, before we can perform the backward construction of the family of co-sliding swap rates, we first need to establish the change of measure, which takes us from the terminal forward LIBOR measure $\mathbb{Q}_n$ to the terminal co-sliding forward swap measure $\mathbb{Q}_{n-N+1}^N$ for a given N. We recall that $\mathbb{Q}_n$ coincides with $\mathbb{Q}_{n-N+1}^N$ for $N = 1$. Hence, we get the following lemma.

Lemma 2. *Under the approximation of the forward swap rate in* (A.26)*, the Radon-Nikodym*

[29] Since the precise drift specification is less relevant for now, we do not write it out explicitly.

derivative of $\mathbb{Q}^N_{n-N+1}$ *with respect to* $\mathbb{Q}_n$ *is*

$$\begin{aligned}\frac{d\mathbb{Q}^N_{n-N+1}}{d\mathbb{Q}_n}_{|\mathcal{F}_t} &\approx \mathcal{E}\left(\int_0^t \varphi_1 dB_s^{\mathbb{Q}_n} + \int_0^t \varphi_2 \sqrt{V_s^W} dW_s^{\mathbb{Q}_n}\right. \\ &\quad + \int_0^t \int_{-\infty}^0 (e^{\varphi_2 x} - 1)\left(\mu^-(dt,dx) - \pi^{\mathbb{Q}_n}_{J^-}(x)dx\nu_t^J dt\right) \\ &\quad \left. + \int_0^t \int_0^\infty (e^{\varphi_2 x} - 1)\left(\mu^+(dt,dx) - \pi^{\mathbb{Q}_n}_{J^+}(x)dx\nu_t^J dt\right)\right), \end{aligned} \tag{A.28}$$

where $\mathcal{E}(\cdot)$ *is the Doléans–Dade exponential and*

$$\begin{aligned}\varphi_1 &= \sum_{k=n-N}^{n-1}\left(\frac{P(0,T_{n-N})}{P(0,T_{n-N}) - P(0,T_n)}\frac{\delta L(0,T_k)}{1+\delta L(0,T_k)} - \tilde{\omega}_k(0)\right)\lambda(s,T_k) \\ \varphi_2 &= \frac{P(0,T_{n-N})}{P(0,T_{n-N}) - P(0,T_n)}\sum_{k=n-N}^{n-1}\frac{\delta L(0,T_k)}{1+\delta L(0,T_k)} - 1.\end{aligned}$$

Proof: Consider the Radon–Nikodym derivative for some $j = 0,\ldots,n-N$ defined by the fraction of the numerators,

$$\frac{d\mathbb{Q}^N_{j+1}}{d\mathbb{Q}_n}_{|\mathcal{F}_t} = \frac{S_t(T_j,T_{j+N})}{P(t,T_n)}\frac{P(0,T_n)}{S_0(T_j,T_{j+N})}, \tag{A.29}$$

which by definition is a $\mathbb{Q}_n$-martingale. We first fix $j = n-N$ for a given N and look at the first term in equation (A.29):

$$\frac{S_t(T_{n-N},T_n)}{P(t,T_n)} = \frac{1}{R^N_{n-N}(t)}\left(\frac{P(t,T_{n-N})}{P(t,T_n)} - 1\right) = \frac{1}{R^N_{n-N}(t)}\left(\prod_{k=n-N}^{n-1}(1+\delta L(t,T_k)) - 1\right). \tag{A.30}$$

By inserting our dynamics of the forward LIBOR rate and the approximate dynamics of the forward swap rate in (A.26), we get, under $\mathbb{Q}_n$,

$$\begin{aligned}\frac{S_t(T_{n-N},T_n)}{P(t,T_n)} &\approx \frac{1}{R^N_{n-N}(0)}\exp\left(-\int_0^t \sum_{k=n-N}^{n-1}\tilde{\omega}_k(0)dX_s + \text{drift}\right) &\text{(A.31)} \\ &\quad \times\left(\prod_{k=n-N}^{n-1}\left[1+\delta L(0,T_k)\exp\left(\int_0^t dX_s + \text{drift}\right)\right] - 1\right) &\text{(A.32)} \\ &\approx \frac{1}{R^N_{n-N}(0)}\frac{P(0,T_{n-N}) - P(0,T_n)}{P(0,T_n)} &\text{(A.33)} \\ &\quad \times\exp\left(\sum_{k=n-N}^{n-1}\int_0^t\left(\frac{P(0,T_{n-N})\frac{\delta L(0,T_k)}{1+\delta L(0,T_k)}}{P(0,T_{n-N}) - P(0,T_n)} - \tilde{\omega}_k(0)\right)dX_s + \text{drift}\right),\end{aligned}$$

by relying (twice) on the approximation $1+\kappa\exp(x) \approx (1+\kappa)\exp(\frac{\kappa}{1+\kappa}x)$ for x small.[30] Inserting

[30] See, e.g., Kluge (2005), page 73.

the definition of the process dX_s under the measure $\mathbb{Q}_n$ proves the proposition. □

Applying the above change of measure result, we get the dynamics of the Lévy components in the proposition. ■

Proof of Proposition 5

For simplicity, we fix $t = 0$. Under some technical conditions,[31] we obtain the Fourier transform of the cap as

$$\begin{aligned}\chi(z) &= \int_{-\infty}^{\infty} e^{izk} C_0(k, T_j)dk = \delta P(0, T_{j+1})\mathbb{E}_0^{Q_{j+1}}\left[\int_{-\infty}^{Y_{T_j}} e^{izk}\left(e^{Y_{T_j}} - e^k\right)dk\right] \\ &= \delta P(0, T_{j+1})\mathbb{E}_0^{Q_{j+1}}\left[\frac{e^{(1+iz)Y_{T_j}}}{iz} - \frac{e^{(1+iz)Y_{T_j}}}{1+iz}\right] = \delta P(0, T_{j+1})\frac{\phi_{Y_{T_j}}(z-i)}{(iz)(iz+1)}, \quad \text{(A.34)}\end{aligned}$$

where $\phi_{Y_{T_j}}(\cdot)$ denotes the characteristic function of Y_{T_j}. Then the option value can be calculated using the Fourier inversion formula:

$$\begin{aligned}C_0(k, T_j) &= \frac{1}{2}\int_{-iz_i-\infty}^{-iz_i+\infty} e^{-izk}\chi(z)dz = \frac{e^{-z_i k}}{\pi}\int_0^{\infty} e^{-iz_r k}\chi(z_r - iz_i)dz_r \\ &= \frac{e^{-z_i k}}{\pi}\delta P(0, T_{j+1})\int_0^{\infty} e^{-iz_r k}\frac{\phi_{Y_{T_j}}(z_r - iz_i - i)}{(iz_r + z_i)(iz_r + z_i + 1)}dz_r \quad \text{(A.35)}\end{aligned}$$

The complex valued measure as developed in Carr and Wu (2004) allows us to write the characteristic function $\phi_{Y_{T_j}}(u) = \mathbb{E}_0^{Q_{j+1}}(\exp(iuY_{T_j}))$ as

$$\begin{aligned}\phi_{Y_{T_j}}(u) &= \mathbb{E}_0^{Q_{j+1}}\left[\exp\left(iu\left(\ln L(0, T_j) + \int_0^{T_j} b(s, T_j, T_{j+1})ds + \int_0^{T_j} dX_s^{Q_{j+1}}\right)\right)\right] \\ &= L(0, T_j)^{iu}\mathbb{E}_0^{\mathbb{Q}_{j+1}}\left[\exp\left(iu\left(\int_0^{T_j} b(s, T_j, T_{j+1})ds + \int_0^{T_j} dX_s^{Q_{j+1}}\right)\right)\right] \\ &= L(0, T_j)^{iu}\mathbb{E}_0^{Q_{j+1}}\left[\exp\left(iu\left(B^{Q_{j+1}}_{\mathcal{T}^B_{T_j}} - \frac{1}{2}\mathcal{T}^B_{T_j}\right) + iu\left(W^{Q_{j+1}}_{\mathcal{T}^W_{T_j}} - \frac{1}{2}\mathcal{T}^W_{T_j}\right)\right.\right. \\ &\quad \left.\left. + iu\left(J^{Q_{j+1}}_{\mathcal{T}^J_{T_j}} - k_J(1)\mathcal{T}^J_{T_j}\right)\right)\right] \\ &= L(0, T_j)^{iu}\mathbb{E}_0^{\mathbb{M}}\left[\exp\left(-\psi_B^{\mathbb{Q}_{j+1}}(u)\mathcal{T}^B_{T_j} - \psi_W^{\mathbb{Q}_{j+1}}(u)\mathcal{T}^W_{T_j} - \psi_J^{\mathbb{Q}_{j+1}}(u)\mathcal{T}^J_{T_j}\right)\right], \quad \text{(A.36)}\end{aligned}$$

where $\psi_B^{\mathbb{Q}_{j+1}}(u)$, $\psi_W^{\mathbb{Q}_{j+1}}(u)$, and $\psi_J^{\mathbb{Q}_{j+1}}(u)$ denote the characteristic exponents of the convexity-adjusted Lévy components and where the time changes are given by

$$\mathcal{T}^B_{T_j} = \int_0^{T_j}\lambda^2(s, T_j)ds, \qquad \mathcal{T}^W_{T_j} = \int_0^{T_j} V_s^W ds, \qquad \mathcal{T}^J_{T_j} = \int_0^{T_j}\nu_s^J ds. \quad \text{(A.37)}$$

[31] See, e.g., Wu (2008).

The change to the measure $\mathbb{M}$ in (A.36) is given by the complex valued exponential $\mathbb{Q}_{j+1}$-martingale,[32]

$$\begin{aligned}\frac{d\mathbb{M}}{d\mathbb{Q}_{j+1}|_{\mathcal{F}_t}} &= \exp\left[iu\left(B^{Q_{j+1}}_{\mathcal{T}^B_{T_j}} - \frac{1}{2}\mathcal{T}^B_{T_j}\right) + \psi_B^{\mathbb{Q}_{j+1}}(u)\mathcal{T}^B_{T_j} + iu\left(W^{Q_{j+1}}_{\mathcal{T}^W_{T_j}} - \frac{1}{2}\mathcal{T}^W_{T_j}\right) + \psi_W^{\mathbb{Q}_{j+1}}(u)\mathcal{T}^W_{T_j}\right. \\ &+ \left. iu\left(J^{Q_{j+1}}_{\mathcal{T}^J_{T_j}} - k_J(1)\mathcal{T}^J_{T_j}\right) + \psi_J^{\mathbb{Q}_{j+1}}(u)\mathcal{T}^J_{T_j}\right] \qquad \text{(A.38)}\end{aligned}$$

for $j = 0, 1 \ldots, n-1$, where $k_J(1)$ represents the cumulant exponent of the Lévy jump component. The advantage of the representation of the characteristic exponent in (A.36) is that we can decompose the problem. First, we need to find the characteristic exponents of the Lévy components prior to the time-change. Second, we need to find the characteristic exponents of the time changes. If all of these parts are analytically tractable, then the characteristic exponent of the time-changed Lévy process is tractable. We start by looking at the terms $\psi_B^{\mathbb{Q}_{j+1}}(u)$ and $\psi_W^{\mathbb{Q}_{j+1}}(u)$ in (A.36), which are the characteristic exponents of the two convexity-adjusted continuous Lévy components $B_t - \frac{1}{2}t$ and $W_t - \frac{1}{2}t$, respectively. Since they do not depend on T_{j+1}, we simplify the notation and get

$$\psi_B(u) = \psi_W(u) = \frac{1}{2}\left(iu + u^2\right). \qquad \text{(A.39)}$$

Next, we determine the characteristic exponent $\psi_J^{\mathbb{Q}_{j+1}}(u)$ of the convexity-adjusted jump component $J_t - k_J(1)t$. For analytical tractability, we adopt the commonly used "freezing of coefficients" approximation:

$$\frac{\delta L(t, T_{n-k})}{\delta L(t, T_{n-k}) + 1} \approx \frac{\delta L(0, T_{n-k})}{\delta L(0, T_{n-k}) + 1}.$$

Then, to determine the approximate characteristic exponent under the appropriate forward measure, $\mathbb{Q}_{j+1}$, we have to compute the integral

$$\psi_J^{\mathbb{Q}_{j+1}}(u) \approx \int_{\mathbb{R}_0}\left(1 - e^{iux}\right)\prod_{k=1}^{n-1-j}\left(1 + \frac{\delta L(0, T_{n-k})}{\delta L(0, T_{n-k}) + 1}\left(e^x - 1\right)\right)\pi_J^{\mathbb{Q}_n}dx \qquad \text{(A.40)}$$

for $j = 0, 1 \ldots, n-1$. Starting from the terminal measure $\mathbb{Q}_n$ (i.e., for $j = n-1$) and given the density describing the arrival rate of jumps, we can calculate the characteristic exponent of the convexity-adjusted jump component:

$$\begin{aligned}\psi_J^{T_n}(u) &= \int_{\mathbb{R}_0}\left(1 - e^{iux}\right)\pi_J^{\mathbb{Q}_n}dx - k_J(1) \\ &= \ln\left((1 - iu\nu_{J^+})(1 + iu\nu_{J^-})\right) - iu\ln\left((1 - \nu_{J^+})(1 + \nu_{J^-})\right). \qquad \text{(A.41)}\end{aligned}$$

[32] We recall that $W^{\mathbb{Q}_{j+1}}_{\mathcal{T}^W_{T_j}}$ denotes the standard Brownian motion W under the T_{j+1}-forward measure and subordinated to the stochastic time-change defined by $\mathcal{T}^W_{T_j}$.

We next consider the characteristic exponent of the convexity-adjusted jump component under the measure $\mathbb{Q}_{n-1}$, i.e., for $j = n-2$. We obtain

$$\begin{aligned}\psi_J^{T_{n-1}}(u) &\approx \int_{\mathbb{R}_0} \left(1 - e^{iux}\right)\left(1 + A_{n-1}\left(e^x - 1\right)\right)\pi_J^{\mathbb{Q}_n} dx - k_J(1) \\ &= (1 - A_{n-1})\ln\left((1 - iu\nu_{J^+})(1 + iu\nu_{J^-})\right) + A_{n-1}\ln\left((1 - iu\nu_{J^+}^{n-2})(1 + iu\nu_{J^-}^{n-2})\right) \\ &\quad -iu\left[(1 - A_{n-1})\ln\left((1 - \nu_{J^+})(1 + \nu_{J^-})\right) + A_{n-1}\ln\left((1 - \nu_{J^+}^{n-2})(1 + \nu_{J^-}^{n-2})\right)\right],\end{aligned}$$

where

$$A_{n-1} = \frac{\delta L(0, T_{n-1})}{\delta L(0, T_{n-1}) + 1}, \quad \nu_{J^+}^j = \frac{\nu_{J^+}}{1 - (n-1-j)\nu_{J^+}}, \quad \nu_{J^-}^j = \frac{\nu_{J^-}}{1 + (n-1-j)\nu_{J^-}}.$$

In the same manner, we can recursively proceed to calculate the characteristic exponents of the convexity-adjusted jump component related to the entire family of forward measures corresponding to the other payment dates $T_1, \ldots, T_{n-2}$ in closed form. It remains to obtain the Laplace transforms of the time changes specified in Section 3.1.1. We start with the deterministic time-change, $\mathcal{T}_{T_j}^B$. We directly obtain

$$\mathbb{E}_0^{\mathbb{M}}\left[\exp\left(-\psi_B^{\mathbb{Q}_{j+1}}(u)\mathcal{T}_{T_j}^B\right)\right] = \exp\left(-\frac{1}{2}\left(iu + u^2\right)\int_0^{T_j}\lambda(s, T_j)^2 ds\right). \tag{A.42}$$

The integral $\int_0^{T_j}\lambda(s, T_j)^2 ds$ results in a lengthy, but closed form expression.[33] Next, we take a look at $\mathcal{T}_t^W$ and $\mathcal{T}_t^J$. Due to the presence of the non-zero correlation parameter, we need to proceed in two steps. First, for the change between the different forward measures, we can rely on the result presented in Proposition 3. Second, when we switch from the forward measure $\mathbb{Q}_{j+1}$ to $\mathbb{M}$, we have to adjust the activity rate dynamics for the time-change $\mathcal{T}_t^W$ as follows,

$$d\widetilde{W}_t^{\mathbb{M}} = = d\widetilde{W}_t^{Q_{j+1}} - \langle d\widetilde{W}_t^{\mathbb{Q}_{j+1}}, iu\sqrt{V_t}dW_t^{T_{j+1}}\rangle = d\widetilde{W}_t^{Q_{j+1}} - iu\sqrt{V_t}\rho dt, \tag{A.43}$$

Finally, we note that the time-change $\mathcal{T}_t^J$ of the jump component remains the same under $\mathbb{M}$ since its driving Brownian motion is assumed to be independent of the different Lévy processes driving the forward LIBOR rate directly. Hence, the activity rates under the measure $\mathbb{M}$ follow the dynamics

$$dV_t^W = \left(\kappa_W\theta_W - \kappa_j^{\mathbb{M}}V_t^W\right)dt + \sigma_W\sqrt{V_t^W}d\widetilde{W}_t^{\mathbb{M}} \tag{A.44}$$

$$d\nu_t^J = \kappa_J(\theta_J - \nu_t^J)dt + \sigma_J\sqrt{\nu_t^J}dZ_t^{\mathbb{M}}, \tag{A.45}$$

[33] The explicit formula can be obtained from the authors.

with $\kappa_j^{\mathbb{M}} = \kappa_W - \sum_{k=1}^{n-j-1} \frac{\delta L(0,T_{n-k})}{1+\delta L(0,T_{n-k})}\sigma_W\rho - iu\sigma_W\rho$ for $j = 0, 1, \ldots, n-1$. As the affine structure is retained, the transform

$$\mathbb{E}_t^{\mathbb{M}}\left[\exp\left(-\psi_W^{\mathbb{Q}_{j+1}}(u)\mathcal{T}_{T_j}^W - \psi_J^{\mathbb{Q}_{j+1}}(u)\mathcal{T}_{T_j}^J\right)\right] \tag{A.46}$$

has the solution

$$\phi^{\mathbb{Q}_{j+1}}(u) \;=\; \exp\left(-a_W(\tau) - b_W(\tau)V_t - a_J(\tau) - b_J(\tau)\nu_t^J\right), \tag{A.47}$$

with the coefficients given in the proposition. Note that $\psi_W(u)$ remains the same regardless of the forward measure under which we perform the pricing and so we omit the dependence on the forward measure for notational convenience. ■

Proof of Proposition 6

For simplicity, we fix $t = 0$. Following the same strategy as for the derivation of the caplet price, the swaption value is

$$PS_0(k, T_j, T_{j+N}) \;\approx\; \frac{e^{-z_i k}}{\pi} S_0(T_j, T_{j+N}) \int_0^\infty e^{-iz_r k} \frac{\phi_{\widetilde{Y}_{T_j}}(z_r - iz_i - i)}{(iz_r + z_i)(iz_r + z_i + 1)} dz_r,$$

where $\phi_{\widetilde{Y}_{T_j}}(z - i)$ denotes the characteristic function of the non-homogenous Lévy process $\widetilde{Y}_{T_j}$ specified under the co-sliding forward swap measure $\mathbb{Q}_{j+1}^N$. The transform $\phi_{\widetilde{Y}_{T_j}}(u)$ takes the form

$$\begin{aligned}
\phi_{\widetilde{Y}_{T_j}}(u) &= \mathbb{E}_0^{\mathbb{Q}_{j+1}^N}\left(\exp\left(iu\widetilde{Y}_{T_j}\right)\right) \\
&= \mathbb{E}_0^{\mathbb{Q}_{j+1}^N}\left[\exp\left(iu\left(\ln R_j^N(0) + \int_0^{T_j}\sum_{k=j}^{j+N-1}\tilde{\omega}_k(0)dX_s^{\mathbb{Q}_{j+1}^N} + \text{drift}\right)\right)\right] \\
&= R_j^N(0)^{iu}\mathbb{E}_0^{\mathbb{Q}_{j+1}^N}\left[\exp\left(iu\left(B_{\mathcal{T}_t^B}^{\mathbb{Q}_{j+1}^N} - \frac{1}{2}\mathcal{T}_{T_j}^B\right) + iu\left(W_{\mathcal{T}_t^W}^{\mathbb{Q}_{j+1}^N} - \frac{1}{2}\mathcal{T}_{T_j}^W\right) + iu\left(J_{\mathcal{T}_{T_j}^J}^{\mathbb{Q}_{j+1}^N} - k_J(1)\mathcal{T}_{T_j}^J\right)\right)\right] \\
&= R_j^N(0)^{iu}\mathbb{E}_0^{\mathbb{M}}\left[\exp\left(-\psi_B^{\mathbb{Q}_{j+1}^N}(u)\mathcal{T}_{T_j}^B - \psi_W^{\mathbb{Q}_{j+1}^N}(u)\mathcal{T}_{T_j}^W - \psi_J^{\mathbb{Q}_{j+1}^N}(u)\mathcal{T}_{T_j}^J\right)\right].
\end{aligned} \tag{A.48}$$

The new measure $\mathbb{M}$ is defined by the complex valued exponential $\mathbb{Q}_{j+1}^N$-martingale,

$$\begin{aligned}
\frac{d\mathbb{M}}{d\mathbb{Q}_{j+1}^N}_{|\mathcal{F}_{t=0}} &= \exp\left[iu\left(B_{\mathcal{T}_{T_j}^B}^{\mathbb{Q}_{j+1}^N} - \frac{1}{2}\mathcal{T}_{T_j}^B\right) + \psi_B^{\mathbb{Q}_{j+1}^N}(u)\mathcal{T}_{T_j}^B + iu\left(W_{\mathcal{T}_{T_j}^W}^{\mathbb{Q}_{j+1}^N} - \frac{1}{2}\mathcal{T}_{T_j}^W\right) + \psi_W^{\mathbb{Q}_{j+1}^N}(u)\mathcal{T}_{T_j}^W\right. \\
&+ \left. iu\left(J_{\mathcal{T}_{T_j}^J}^{\mathbb{Q}_{j+1}^N} - k_J(1)\mathcal{T}_{T_j}^J\right) + \psi_J^{\mathbb{Q}_{j+1}^N}(u)\mathcal{T}_{T_j}^J\right]
\end{aligned} \tag{A.49}$$

for $j = 0, \ldots, n-N$. Since by construction we have $\sum_{k=j}^{j+N-1} \frac{\omega_k(0)L(0,T_k)}{R_j^N(0)} = 1$, the weights have no impact on the stochastic time changes to the Brownian motion W and the jump component J because these time changes do not depend on the particular maturity T_k. Hence, the time changes now become

$$\mathcal{T}_{T_j}^B = \int_0^{T_j} \left(\sum_{k=j}^{j+N-1} \tilde{\omega}_k(0)\lambda(s,T_k) \right)^2 ds, \qquad \mathcal{T}_{T_j}^W = \int_0^{T_j} V_s^W ds, \qquad \mathcal{T}_{T_j}^J = \int_0^{T_j} \nu_s^J ds \tag{A.50}$$

The pricing problem can now be split again into calculating the characteristic exponents prior to the time changes and the characteristic exponent of the time changes. The characteristic exponents of the two convexity-adjusted continuous Lévy components prior to the time-change remain the same as in the LIBOR model setting. To determine $\psi_J^{\mathbb{Q}_{j+1}^N}(u)$, we first look at the jump intensity under the co-sliding forward measure $\mathbb{Q}_{j+1}^N$. It is related to the jump intensity under the terminal co-sliding forward measure $\mathbb{Q}_{n-N+1}^N$ by

$$\pi_J^{\mathbb{Q}_{j+1}^N} \nu_t^J \approx \prod_{k=1}^{n-N-j} \left(1 + \frac{\delta R_{n-N+1-k}^N(0)}{1 + \delta R_{n-N+1-k}^N(0)} \left(e^x - 1 \right) \right) \pi_J^{\mathbb{Q}_{n-N+1}^N} \nu^J, \tag{A.51}$$

where $j = 0, 1 \ldots, n-N$ and

$$\pi_J^{\mathbb{Q}_{n-N+1}^N}(x) = \begin{cases} \lambda e^{-\frac{|x|}{\bar{\nu}_+}} |x|^{-1}, & x > 0 \\ \lambda e^{-\frac{|x|}{\bar{\nu}_-}} |x|^{-1}, & x < 0 \end{cases}, \tag{A.52}$$

with

$$\bar{\nu}_+ = \frac{\nu_+}{1 - \varphi_2 \nu_+}, \quad \bar{\nu}_- = \frac{\nu_-}{1 + \varphi_2 \nu_-}. \tag{A.53}$$

Note that we require $\lambda, \bar{\nu}_+, \bar{\nu}_- > 0$. By inspection of (A.52), we see that the change of measure from the terminal forward LIBOR measure to the co-sliding terminal swap measure is driven by the term φ_2. Clearly, when $N = 1$, we are back in our LIBOR market setting. Next, as in equation (A.40) for the LIBOR specification, we freeze coefficients and set

$$\frac{\delta R_{n-N+1-k}^N(t)}{1 + \delta R_{n-N+1-k}^N(t)} \approx \frac{\delta R_{n-N+1-k}^N(0)}{1 + \delta R_{n-N+1-k}^N(0)},$$

to obtain

$$\begin{aligned} \psi_J^{\mathbb{Q}_{j+1}^N}(u) &= \int_{\mathbb{R}_0} \left(1 - e^{iux}\right) \prod_{k=1}^{n-N-j} \left(1 + \gamma_J(t, T_{n-N+1-k}, T_{n+1-k})\right) \pi_J^{\mathbb{Q}_{n-N+1}^N} dx \\ &\approx \int_{\mathbb{R}_0} \left(1 - e^{iux}\right) \prod_{k=1}^{n-N-j} \left(1 + \frac{\delta R_{n-N+1-k}^N(0)}{1 + \delta R_{n-N+1-k}^N(0)} \left(e^x - 1 \right) \right) \pi_J^{\mathbb{Q}_{n-N+1}^N} dx, \end{aligned} \tag{A.54}$$

for $j = 0, 1 \ldots, n-N$. Because $R^N_{n-N}(t)$ is a $\mathbb{Q}^N_{n-N+1}$-martingale, we obtain, for $j = n-N$,

$$\begin{aligned}\psi_J^{\mathbb{Q}^N_{n-N+1}}(u) &= \int_{\mathbb{R}_0} \left(1 - e^{iux}\right) \pi_J^{\mathbb{Q}^N_{j+1}} dx - k_J^{n-N}(1) \\ &= \ln\left((1 - iu\bar{\nu}_{J^+})(1 + iu\bar{\nu}_{J^-})\right) - iu \ln\left((1 - \bar{\nu}_{J^+})(1 + \bar{\nu}_{J^-})\right). \qquad \text{(A.55)}\end{aligned}$$

Equation (A.55) is similar to the characteristic exponent in (A.41) for the LIBOR rate, but with $k_J^{n-N}(s)$ as the cumulant exponent of the Lévy jump component with the adjusted jump parameters given in (A.53). Next, we note that for a given N we have a family of co-sliding forward swap measures denoted by $\left\{\mathbb{Q}^N_1, \mathbb{Q}^N_2 \ldots, \mathbb{Q}^N_{n-N+1}\right\}$. To find the characteristic exponent of the convexity-adjusted jump component $\psi_J^{\mathbb{Q}^N_{n-N}}(u)$ related to the swap measure $\mathbb{Q}^N_{n-N}$ prior to the time-change, we have to adjust the (co-sliding terminal) Lévy density exactly as we did in the LMM. Working back recursively, and since $R^N_{n-N-1}(t)$ is a $\mathbb{Q}^N_{n-N}$-martingale, we get, for $j = n-N-1$,

$$\begin{aligned}\psi_J^{\mathbb{Q}^N_{n-N}}(u) &\approx \int_{\mathbb{R}_0} \left(1 - e^{iux}\right) \left(1 + A_{n-N}\left(e^x - 1\right)\right) \pi_J^{\mathbb{Q}^n_{n-N+1}} dx - k_J^{n-N-1}(1) \\ &= (1 - A_{n-N}) \ln\left((1 - iu\bar{\nu}_{J^+})(1 + iu\bar{\nu}_{J^-})\right) + A_{n-N} \ln\left((1 - iu\bar{\nu}_{J^+}^{n-N-1})(1 + iu\bar{\nu}_{J^-}^{n-N-1})\right) \\ &\quad -iu\left[(1 - A_{n-N}) \ln\left((1 - \bar{\nu}_{J^+})(1 + \bar{\nu}_{J^-})\right) + A_{n-N} \ln\left((1 - \bar{\nu}_{J^+}^{n-N-1})(1 + \bar{\nu}_{J^-}^{n-N-1})\right)\right],\end{aligned}$$

where

$$A_{n-N} = \frac{\delta R^N_{n-N}(0)}{1 + \delta R^N_{n-N}(0)}, \quad \bar{\nu}^j_{J^+} = \frac{\bar{\nu}_{J^+}}{1 - (n-N-j)\bar{\nu}_{J^+}}, \quad \bar{\nu}^j_{J^-} = \frac{\bar{\nu}_{J^-}}{1 + (n-N-j)\bar{\nu}_{J^-}}.$$

Following the same argument, we can calculate the characteristic exponents of the convexity-adjusted jump component related to the other co-sliding swap measures $\left\{\mathbb{Q}^N_1, \mathbb{Q}^N_2, \ldots, \mathbb{Q}^N_{n-N-1}\right\}$ in closed form.

As in to the LIBOR market setting, we can show that the activity rate dynamics under the complex measure $\mathbb{M}$ obeys the following form,

$$dV_t^W = \left(\kappa_W \theta_W - \kappa_j^{\mathbb{M}} V_t^W\right) dt + \sigma_W \sqrt{V_t^W} d\widetilde{W}_t^{\mathbb{M}} \qquad \text{(A.56)}$$

$$d\nu_t^J = \kappa_J(\theta_J - \nu_t^J)dt + \sigma_J \sqrt{\nu_t^J} dZ_t^{\mathbb{M}}, \qquad \text{(A.57)}$$

with $\kappa_j^{\mathbb{M}} = \kappa_W - \varphi_2 \sigma_W \rho - \sum_{k=1}^{n-N-j} \frac{\delta R^N_{n-N+1-k}(0)}{1+\delta R^N_{n-N+1-k}(0)} \sigma_W \rho - iu\sigma_W \rho$ for $j = 0, 1, \ldots, n-N$.[34] Since

[34] Note that all the change of measure results applied to the co-sliding swap market model should match the formulae presented for the LMM in the case $N = 1$ corresponding to a co-sliding forward swap rate defined on a three months tenor, in which case it equals the definition of the forward LIBOR rate.

the time-change $\mathcal{T}_t^B$ is deterministic, we obtain

$$\mathbb{E}_0^{\mathbb{M}}\left[\exp\left(-\psi_B^{\mathbb{Q}_{j+1}^N}(u)\mathcal{T}_{T_j}^B\right)\right] = \exp\left(-\frac{1}{2}\left(iu+u^2\right)\int_0^{T_j}\left(\sum_{k=j}^{j+N-1}\tilde{\omega}_k(0)\lambda(s,T_k)\right)^2 ds\right),$$

which can be computed in closed form. We are therefore left with the Laplace transform

$$\mathbb{E}_0^{\mathbb{M}}\left[\exp\left(-\psi_W^{\mathbb{Q}_{j+1}^N}(u)\mathcal{T}_{T_j}^W - \psi_J^{\mathbb{Q}_{j+1}^N}(u)\mathcal{T}_{T_j}^J\right)\right]. \tag{A.58}$$

Due to its exponential affine structure, the Laplace transform has a closed form solution:

$$\phi(u) = \exp\left(-a_W(\tau) - b_W(\tau)V_t - a_J(\tau) - b_J(\tau)\nu_t^J\right), \qquad \tau = T_j - t, \tag{A.59}$$

with

$$a_i(\tau) = \frac{\kappa_i\theta_i}{\sigma_i^2}\left[2\ln\left(1-\frac{\gamma_i-\hat{\kappa}_i}{2\gamma_i}\left(1-e^{-\gamma_i\tau}\right)\right)+\left(\gamma-\hat{\kappa}_i\right)\tau\right] \tag{A.60}$$

$$b_i(\tau) = \frac{2\psi_i(u)\left(1-e^{-\gamma_i\tau}\right)}{2\gamma_i-\left(\gamma_i-\hat{\kappa}_i\right)\left(1-e^{-\gamma_i\tau}\right)}, \qquad \gamma_i = \sqrt{\hat{\kappa}_i^2+2\sigma_i^2\psi_i(u)}, \tag{A.61}$$

for

$$\psi_i(u) = \begin{cases} \psi_W(u) & \text{if } i = W \\ \psi_J^{\mathbb{Q}_{j+1}^N}(u) & \text{if } i = J \end{cases}, \qquad \hat{\kappa}_i = \begin{cases} \bar{\kappa}_j^{\mathbb{M}} & \text{if } i = W \\ \kappa_J & \text{if } i = J \end{cases}.$$

The index j denotes the option maturity under consideration.

Appendix B

In this appendix, we describe how we transformed the market quotes into the option prices that we used for our model estimation.

Market prices of caps and floors

Given an implied volatility quote $IV(t,T,K)$ at time t for a cap with maturity date T, strike rate K, and tenor δ, the invoice (dollar) price of the cap with one dollar principal is computed based on Black's formula, Black (1976),

$$\text{Cap}_t(T,K) = \sum_{i=1}^{N} C_t(T_i,K) = \delta\sum_{i=1}^{N} P(t,t+(i+1)\delta)\left[L(t,t+i\delta)N(d_{1i}) - KN(d_{2i})\right] \tag{A.62}$$

where $T = (N+1)\delta$. Here, $C_t(T,K)$ is the price of the caplet with maturity $T-t$ and strike K, $P(t,T)$ denotes the zero-coupon bond with time to maturity $T-t$, and $L(t,T)$ denotes the forward LIBOR rate at time t for $[T, T+\delta]$. Also, $N(\cdot)$ denotes the cumulative normal density, and d_{1i} and d_{2i} are defined by

$$d_{1i} = \frac{\ln(L(t,t+i\delta)/K) + IV^2(i\delta)/2}{IV\sqrt{i\delta}}, \quad d_{2i} = d_{1i} - IV\sqrt{i\delta}. \tag{A.63}$$

Caplets are paid in arrears. The payoff settled at time T is to be paid one tenor later at $T+\delta$. For U.S. dollar caps and floors, the payment interval is three months, i.e., $\delta = 1/4$. From the Black-implied cap prices, the price of a floor contract can be computed by the parity,

$$\text{Cap}_t(T,K) - \text{Floor}_t(T,K) \quad = \quad \text{Payer Swap}_t(T,K) \tag{A.64}$$

which implies that

$$\text{Floor}_t(T,K) \quad = \quad \text{Cap}_t(T,K) + \sum_{i=1}^{N} \delta P(t,t+(i+1)\delta)(K - L(t,t+i\delta)), \tag{A.65}$$

where the second term on the right hand side is simply the present value of a (receiver) swap contract. For the estimation of our model, we normalized the option prices by their vega, i.e., their sensitivity to volatility changes. For caps (and floors) the vega is given by

$$\mathcal{V}_{cap/floor} \equiv \frac{\partial Cap/Floor}{\partial IV} \quad = \quad \delta \sum_{i=1}^{N} P(t,t+(i+1)\delta) L(t,t+i\delta) N'(d_{1i}) \sqrt{i\delta}. \tag{A.66}$$

Market prices of payer and receiver swaptions

Given an ATM implied swaption volatility quote $IV(t,T_j,T_{j+N})$ at time t for an option expiry at time T_j and a swap tenor equal to $T_N - T_j$ and tenor δ, the invoice (dollar) price of a payer swaption can be computed by relying on the Black (1976) formula for swaptions. In particular, the price for a $T_j \times (T_{j+N} - T_j)$ payer swaption at time t becomes

$$\text{Payer Swaption}_t(T_j,T_{j+N}) \quad = \quad S(t,T_j,T_{j+N}) \left[R(t,T_j,T_{j+N}) N(d_1) - K N(d_2) \right], \tag{A.67}$$

where

$$d_1 = \frac{\ln(R(t,T_j,T_{j+N})/K) + \frac{1}{2} IV(t,T_j,T_{j+N})^2 (T_j - t)}{IV(t,T_j,T_{j+N})\sqrt{T_j - t}}, \quad d_2 = d_1 - IV(t,T_j,T_{j+N})\sqrt{T_j - t}. \tag{A.68}$$

Furthermore, $S(t,T_j,T_{j+N}) = \sum_{k=j+1}^{j+N} \delta P(t,T_k)$ and the underlying forward swap rate can be computed by $R(t,T_j,T_{j+N}) = \frac{P(t,T_j)-P(t,T_{j+N})}{S(t,T_j,T_{j+N})}$. From the payer swaption prices, one can apply the parity to obtain receiver swaption prices:

$$\text{Payer Swaption}(t,T_j,T_{j+N}) - \text{Receiver Swaption}(t,T_j,T_{j+N}) \quad = \quad \text{Payer Swap}(t,T_j,T_{j+N}) \tag{A.69}$$

Here, the Payer Swap can be represented by $S(t,T_j,T_{j+N})(R(t,T_j,T_{j+N}) - K)$. Similarly to Caps/Floors, the ATM swaption strike is defined to be the value of K which makes the payer swaption and receiver swaption prices equal to each other. From this parity relation, it follows that the ATM strike rate is simply the forward starting par swap rate given by $R(t,T_j,T_{j+N})$. For payer and receiver swaptions, we have a formula for the vega:

$$\mathcal{V}_{Swaption} \equiv \frac{\partial Swaption}{\partial IV} \quad = \quad S(t,T_j,T_{j+N})R(t,T_j,T_{j+N})N'(d_1)\sqrt{T_j - t}. \tag{A.70}$$

As for caps, we normalized the swaption prices by their Black (1976) vega.

Table 1
Principal component analysis.

	Number of term structure and volatility factors (m, n)							
	(1,1)	(1,2)	(2,1)	(2,2)	(2,3)	(3,1)	(3,2)	(3,3)
Caps	89.7	94.9	93.3	97.4	98.0	95.0	97.7	98.3
ATM swaptions	89.6	92.0	91.2	93.8	94.6	94.1	95.9	96.6
Non-ATM swaptions	86.0	89.2	87.7	92.0	93.6	91.6	94.6	96.1
Total	88.5	92.1	90.8	94.4	95.4	93.6	96.1	97.0

R^2 values (in percentages) from regressing the implied volatilities of caps and swaptions on the yield curve factors and the volatility factors. We obtain the yield curve factors from a PCA on LIBOR and swap rates. The volatility factors are obtained from a PCA on the residuals of regressing the implied volatilities on the yield curve factors. The table shows the R^2 values (in percentage) for different factor combinations (m, n), where m is the number of yield curve factors and n is the number of volatility factors. The numbers are averaged for caps, ATM swaptions, and non-ATM swaptions. We base our analysis on weekly data sampled on Wednesdays, spanning the period August 8, 2007 to August 11, 2011.

Table 2
Explained variation for swaptions across option maturities and swap tenors for the (3,2)-model.

Panel A: R^2 for ATM swaptions

	Option maturity								
Swap tenor	3 m	6 m	1 y	2 y	3 y	4 y	5 y	7 y	10 y
1 y	94.4	97.0	97.4	95.4	95.9	95.3	95.1	94.3	91.9
2 y	94.9	96.7	96.3	95.7	96.0	95.7	95.7	95.4	92.1
3 y	95.6	96.1	96.9	96.8	96.5	96.5	96.1	96.0	91.4
4 y	95.4	96.8	97.8	97.4	97.2	97.0	96.6	96.0	90.8
5 y	95.1	97.4	98.1	97.7	97.6	97.3	96.9	95.7	90.3
7 y	96.5	97.9	98.4	97.8	97.6	97.2	96.7	95.1	90.8
10 y	95.8	97.0	97.7	97.4	97.1	96.6	95.9	94.2	91.3

Panel B: R^2 for non-ATM swaptions

	Option maturity				*Swap tenor*		
Moneyness	3 m	1 y	5 y	10 y	2 y	5 y	10 y
0.90	93.1	97.3	96.0	90.0	92.6	94.8	94.9
0.95	93.3	97.5	96.2	91.0	93.1	95.3	95.2
1.05	93.5	97.6	96.3	91.7	93.4	95.6	95.3
1.10	93.5	97.5	96.2	92.2	93.6	95.8	95.3

Panel A shows the R^2 values from regressing the (3,2)-model with three term structure and two volatility factors on ATM swaptions volatilities. Panel B shows the corresponding R^2 values for non-ATM volatilities. We base our analysis on weekly data sampled on Wednesdays, spanning the period August 8, 2007 to August 11, 2011.

Table 3
Parameter Estimates.

κ_W	0.021	(0.000)	κ_J	0.773	(0.594)	θ_W	0.065	(0.005)	θ_J	0.083	(0.058)
σ_W	0.773	(0.000)	σ_J	2.263	(0.066)	ν_+	0.016	(0.000)	ν_-	0.018	(0.000)
γ^V	-0.064	(0.033)	γ^ν	-0.531	(0.000)	β_1	0.278	(0.004)	β_2	0.023	(0.019)
β_3	0.666	(0.000)	β_4	0.085	(0.006)	ρ	-0.844	(0.000)	σ_e^2	0.001	(0.000)
$\mathcal{L}$	-49,598										

Maximum likelihood estimates of the model parameters, their standard errors (in parentheses), and the log-likelihood value denoted by $\mathcal{L}$. We estimate our model on weekly data sampled on Wednesdays, spanning the period August 8, 2007 to August 11, 2010.

Table 4
Pricing errors for the caps market

	RMSE					MPE				
Maturity	0.80	0.90	1.00	1.10	1.20	0.80	0.90	1.00	1.10	1.20
1 y	16.86	18.62	20.15	20.30	22.03	-10.73	-11.08	-11.95	-12.32	-15.96
2 y	12.26	11.71	9.79	9.57	9.85	-8.64	-8.77	-6.99	-6.17	-7.01
3 y	8.78	6.75	4.75	4.19	4.02	-6.67	-5.15	-3.44	-2.52	-2.59
4 y	6.47	4.29	2.25	1.66	2.03	-4.81	-2.98	-1.40	-0.48	-0.06
5 y	4.98	2.94	1.35	1.26	2.18	-3.41	-1.67	-0.30	0.56	1.29
6 y	4.28	2.36	1.41	1.68	2.50	-2.63	-0.92	0.31	1.11	1.97
7 y	3.91	2.16	1.71	2.08	2.71	-2.07	-0.38	0.74	1.48	2.25
8 y	3.63	2.07	1.89	2.27	2.80	-1.71	-0.07	0.95	1.63	2.33
9 y	3.48	2.09	2.04	2.42	2.88	-1.35	0.20	1.15	1.79	2.41
10 y	3.37	2.15	2.18	2.54	2.95	-1.06	0.42	1.31	1.91	2.47

Sample averages of the root mean squared (RMSE) and mean pricing errors (MPE) for caps implied volatilities, defined as the difference in percentage points between the model-implied values and the market-implied volatility quotes. Each column represents one cap maturity and rows represent the moneyness of the cap.

Table 5: Pricing errors for ATM swaptions

		RMSE							MPE						
Swap tenor:		1 y	2 y	3 y	4 y	5 y	7 y	10 y	1 y	2 y	3 y	4 y	5 y	7 y	10 y
Option	3 m	21.16	9.66	4.46	4.82	5.94	8.30	10.32	-14.13	-7.24	-1.97	0.72	1.77	5.09	7.38
maturity:	6 m	19.53	7.93	2.58	2.60	3.78	6.17	7.89	-13.67	-6.05	-1.45	0.90	1.93	4.35	6.10
	1 y	12.72	5.27	1.74	1.52	2.27	3.82	4.95	-8.81	-3.21	-0.43	0.86	1.48	2.83	3.84
	2 y	4.20	2.20	1.49	1.31	1.36	1.61	2.04	-1.03	0.15	0.61	0.71	0.65	0.75	1.13
	3 y	2.34	1.75	1.38	1.18	1.13	1.22	1.41	1.33	1.16	0.86	0.51	0.16	-0.05	-0.03
	4 y	2.36	1.65	1.29	1.08	1.19	1.25	1.40	1.85	1.20	0.71	0.14	-0.17	-0.53	-0.65
	5 y	2.36	1.65	1.35	1.25	1.32	1.51	1.67	1.89	1.13	0.49	-0.07	-0.47	-0.73	-0.88
	7 y	2.10	1.53	1.36	1.32	1.32	1.54	1.80	1.44	0.73	0.28	-0.16	-0.44	-0.74	-1.07
	10 y	1.93	1.56	1.40	1.39	1.42	1.53	1.72	1.32	0.88	0.50	0.22	-0.01	-0.47	-0.76

Sample averages of the root mean squared (RMSE) and mean pricing errors (MPE) for ATM swaptions implied volatilities, defined as the difference in percentage points between the model-implied values and the market-implied volatility quotes. Each column represents one swaption maturity and each row represent swap tenor.

Table 6
Pricing errors for non-ATM swaptions

Maturities:		RMSE				MPE			
Option	*Swap*	0.90	0.95	1.05	1.10	0.90	0.95	1.05	1.10
3 m	2 y	1.72	10.69	7.39	13.28	-0.76	-7.89	2.24	4.82
3 m	5 y	11.37	12.09	5.26	12.59	-8.33	-8.52	1.01	9.44
3 m	10 y	9.66	11.79	4.92	9.64	-7.47	5.95	0.41	6.77
1 y	2 y	9.79	5.81	2.76	7.37	6.73	-3.43	1.62	6.02
1 y	5 y	5.01	6.41	1.51	5.96	-3.50	-3.57	0.97	4.41
1 y	10 y	5.05	3.81	1.19	4.27	-3.31	2.03	0.66	3.35
5 y	2 y	3.76	1.87	1.48	2.23	2.94	1.31	-0.79	-1.50
5 y	5 y	1.25	2.17	1.35	1.78	0.33	1.55	-0.31	-1.15
5 y	10 y	1.36	1.83	1.46	1.51	0.71	-1.17	-0.15	-0.79
10 y	2 y	1.54	1.86	1.62	2.45	-0.70	1.24	-0.53	-1.77
10 y	5 y	1.50	2.15	1.49	2.02	-0.31	1.58	0.26	-1.24
10 y	10 y	1.43	1.97	1.59	1.67	0.32	-1.09	0.55	-0.52

Sample averages of the root mean squared (RMSE) and mean pricing errors (MPE) for non-ATM swaptions implied volatilities, defined as the difference in percentage points between the model-implied values and the market-implied volatility quotes. Each column represents one swaption maturity and one swap tenor. Each row represents one level of moneyness.

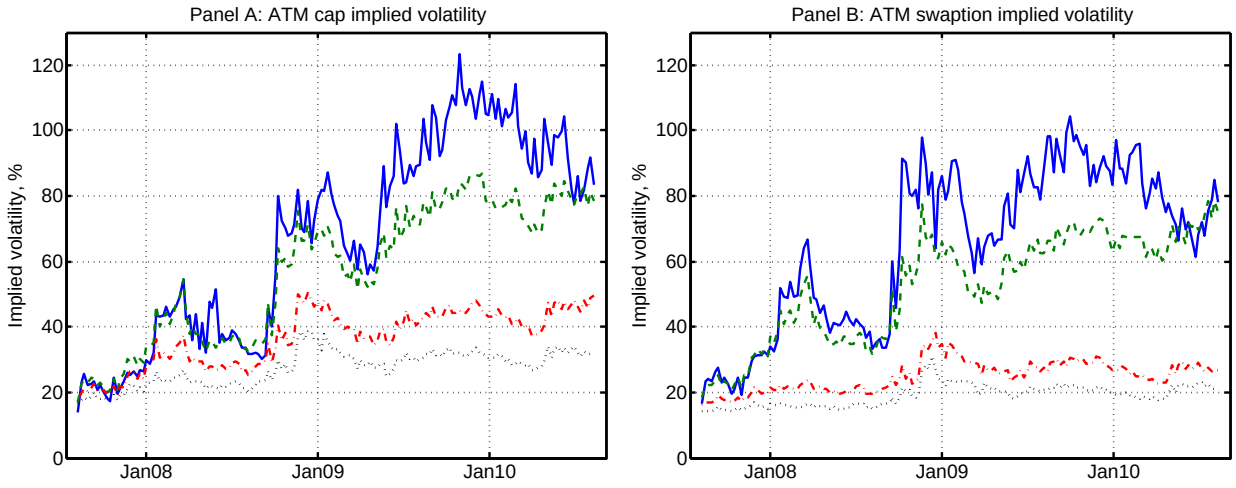

Figure 1. Time-variation in caps and swaptions ATM implied volatilities. The figure shows the time-variation in ATM cap (Panel A) and swaption (Panel B) implied volatilities. For caps, we use option maturities of one (solid line), two (dashed line), five (dash-dotted line), and ten years (dotted line). For swaptions, we use option maturities of three months, one year, five years, and ten years, for a one year swap term. The data are weekly (Wednesday), spanning our entire data sample from August 8, 2007 to August 11, 2010, in total, 158 weeks.

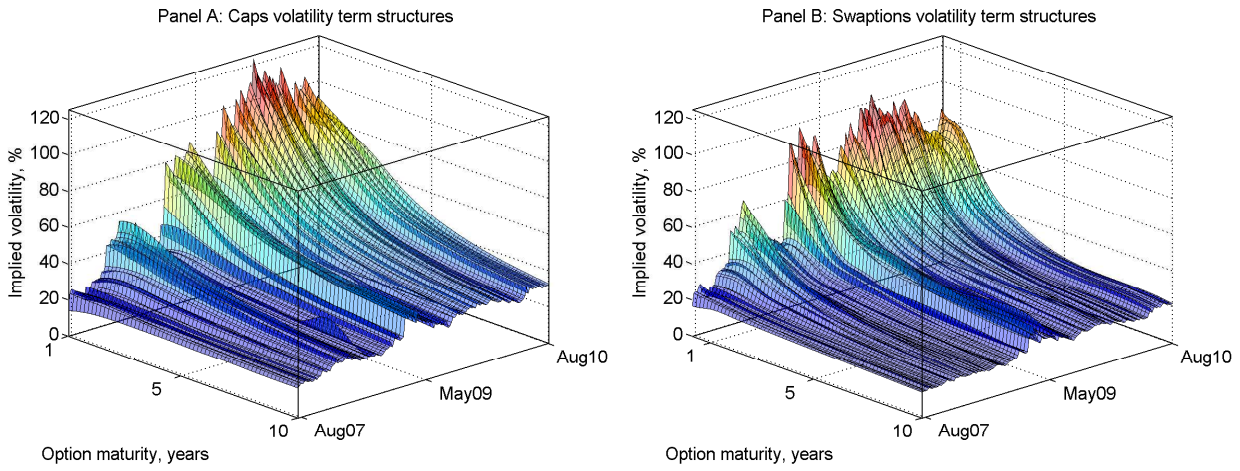

Figure 2. Evolution of implied volatility term structures. Panel A shows the evolution of the ATM volatility term structure for caps implied volatilities across the one to ten years option maturities. Panel B shows the evolution of the ATM volatility term structure for swaptions implied volatilities across the three months to ten year option maturities for the one year swap tenor.

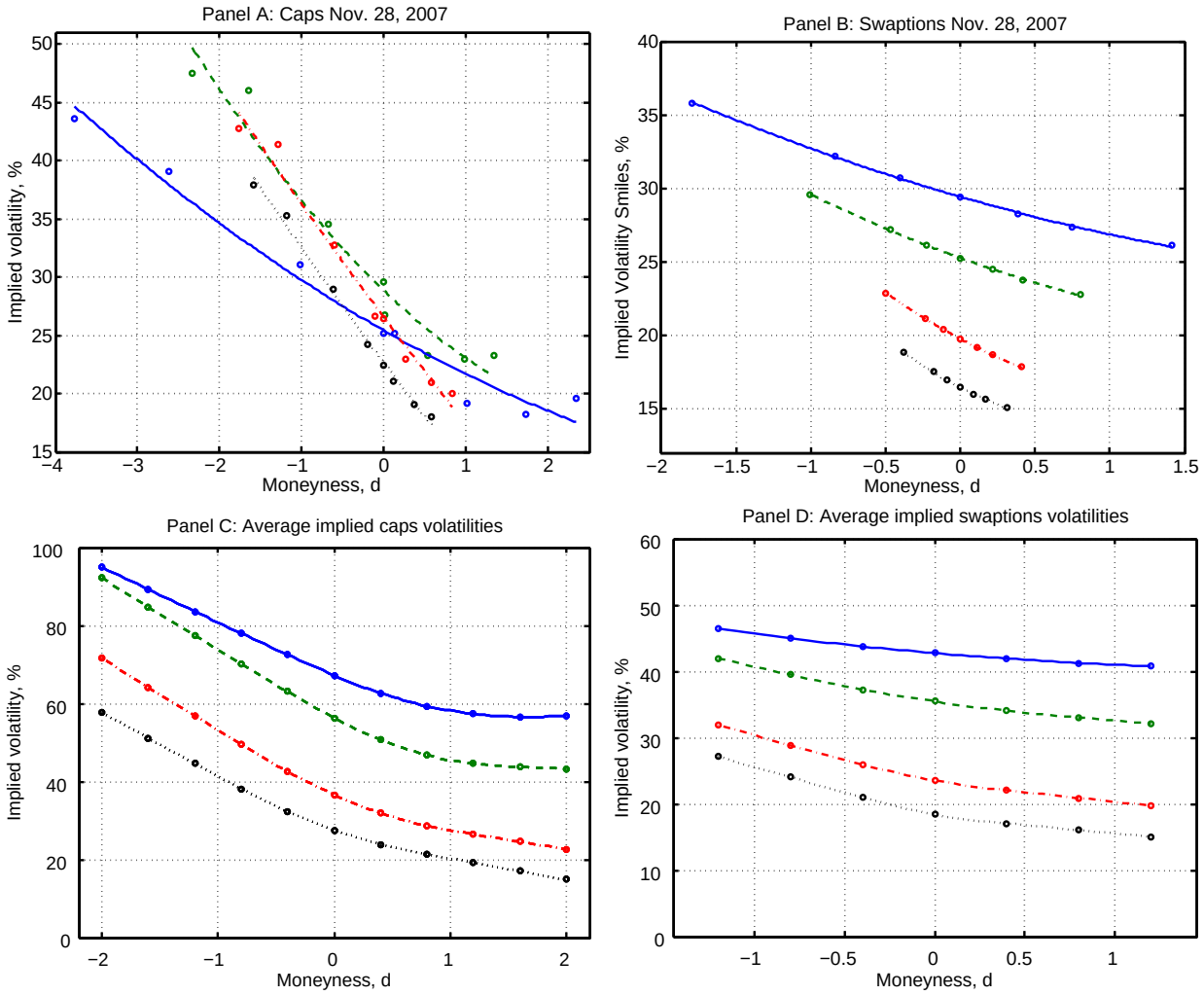

Figure 3. Cap and swaptions implied volatility smiles and skews across moneyness. In Panel A, we plot caps implied volatility smiles on November 28, 2007. The four lines in Panel A correspond to four maturities: one year (solid line), two years (dashed line), five years (dash-dotted line), and ten years (dotted line). Circles are data points, lines are quadratic fits. In Panel B, we plot swaptions implied volatility smiles on November 28, 2007, for a five year swap tenor. The four lines in each panel represent four option maturities: three months (solid line), one year (dashed line), five years (dash-dotted line), and ten years (dotted line). In Panels C and D, we plot the corresponding implied volatility smiles for caps and swaptions when averaged across our whole data sample.

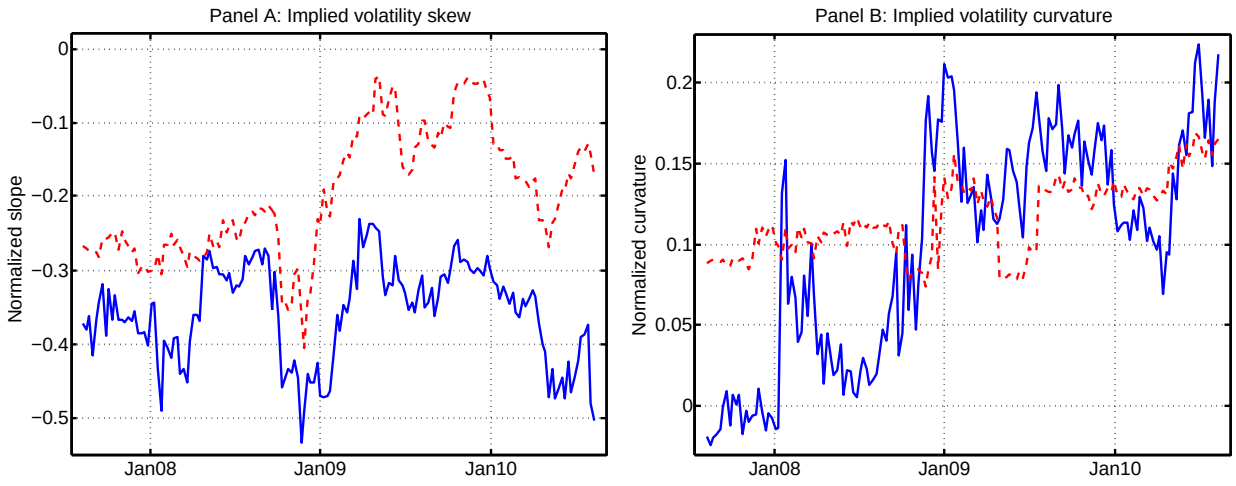

Figure 4. Time-variation in caps and swaptions implied volatility skew and curvature. The figure plots the time series of the slope and curvature of the caps and swaptions implied volatility smile. In Panel A, we plot the implied volatility skew of a five year cap (solid line) and for a five year swaption to enter into a two year swap (dotted line). In Panel B we plot, for the same contracts, the time series of the corresponding curvatures. The caps and swaptions skews and curvatures have been fitted using weekly (Wednesday) data, spanning the period from August 8, 2007 to August 11, 2010.

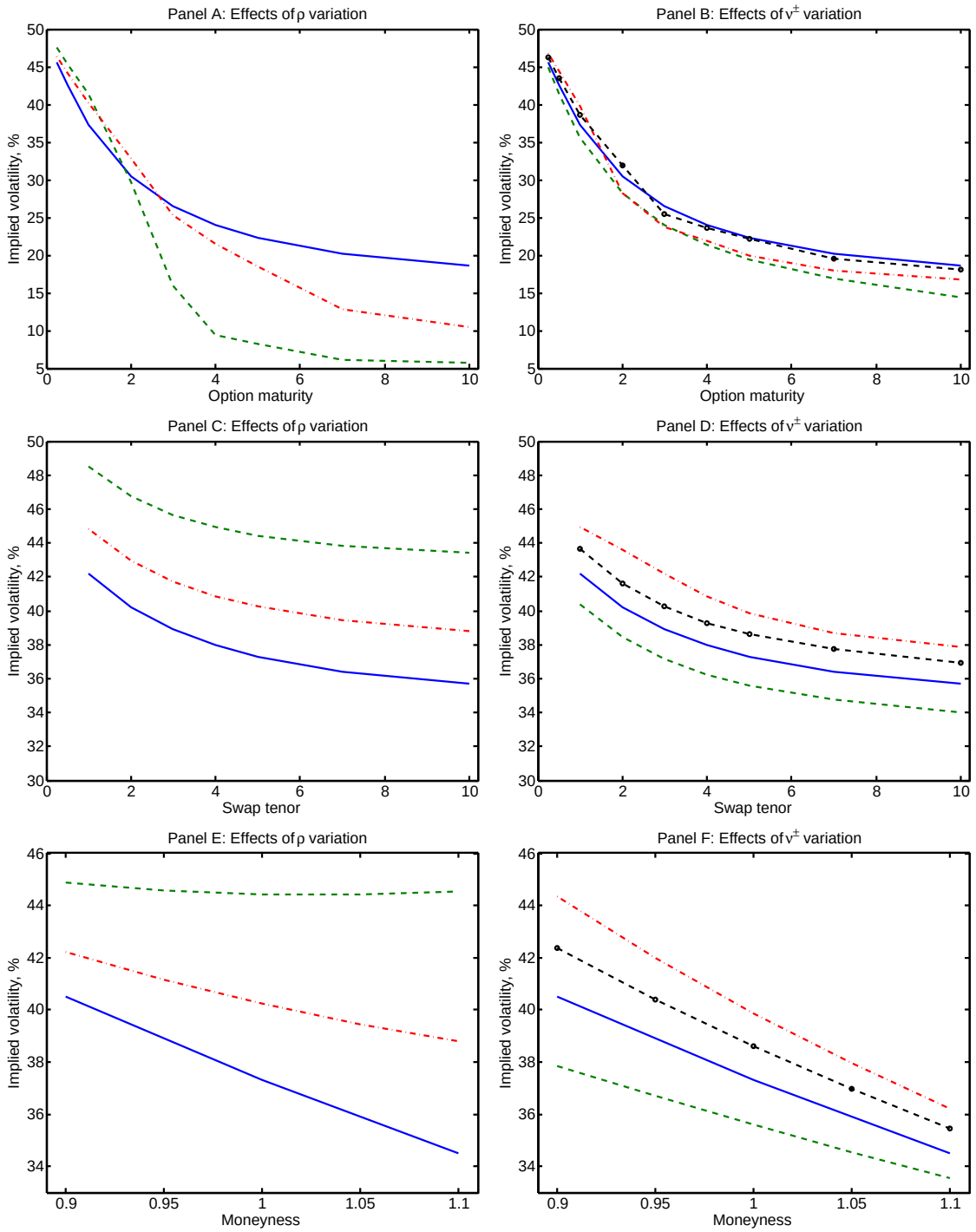

Figure 5. Response of swaption implied volatilities. Solid lines in each panel plot implied volatilities with all parameters set equal to their estimated values and the activity rates set equal to their sample averages. We fix the swap tenor to five years and/or the option maturity to one year. Panels A and B show the responses of the swaption implied volatility to changes in ρ and $\nu^{\pm}$ as a function of the option maturity. In Panels A, C, and D the dashed lines represent the case $\rho =$ and the dash-dotted lines the case $\rho = -0.5$. In Panels B, D, and F the dashed lines correspond to $(\nu^{+} = 0.05, \nu^{-} = 0)$, the dash-dotted lines to $(\nu^{+} = 0, \nu^{-} = 0.05)$, and the dashed lies with dots as markers to $(\nu^{+} = 0.05, \nu^{-} = 0.05)$. For Panels A to D we use ATM swaptions.

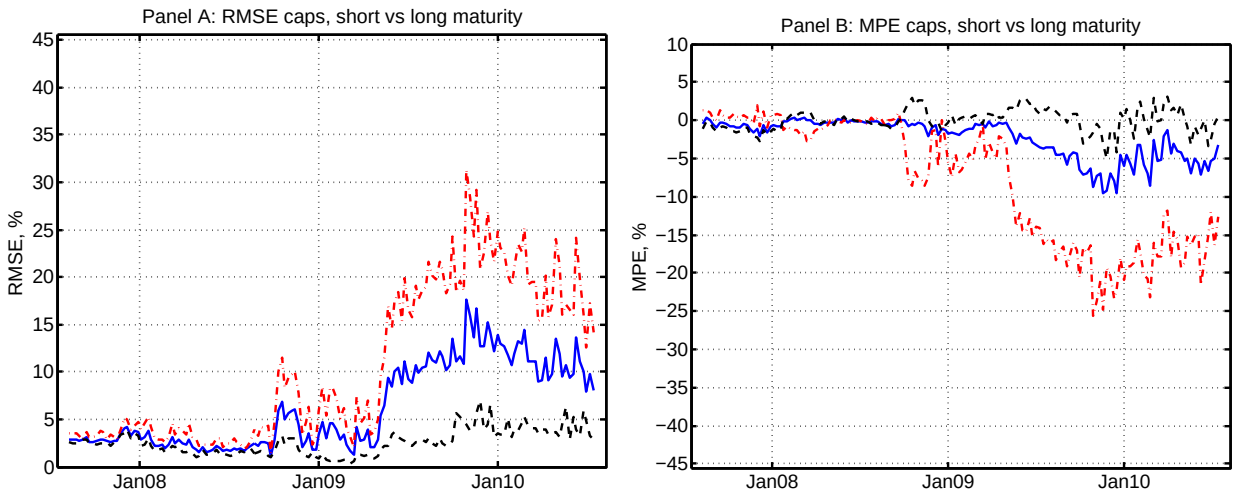

Figure 6. RMSE and MPE for caps with different option maturities. Panels A and B show the RMSE and the MPE across time for caps implied volatilities of all maturities (solid line), for maturities up to three years (dash-dotted line), and for maturities of four to ten years (dashed line). Data are weekly (Wednesday) spanning our entire data sample August 8, 2007 to August 11, 2010, in total 158 weeks.

Figure 7. RMSE and MPE for swaptions with different option maturities and swap tenors. Panels A and B show the RMSE and the MPE for swaptions implied volatilities of all tenors (solid line), for tenors up to three years (dash-dotted line), and for tenors of four to ten years (dashed line). In Panels C and D, we plot the RMSE and MPE for swaptions implied volatilities with short option maturities up to two years (dash-dotted line), and for option maturities of three to ten years (dashed line). Furthermore, in Panel D we plot the MPE for implied volatilities of swaptions with short option maturity and short swap tenor (dotted line). Data are weekly (Wednesday) spanning our entire data sample August 8, 2007 to August 11, 2010, in total 158 weeks.

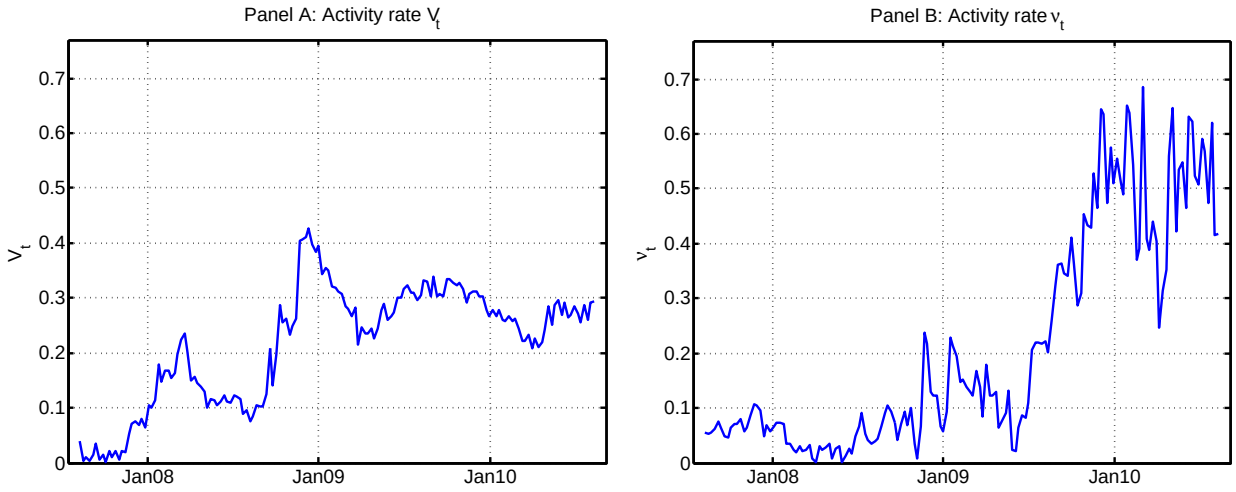

Figure 8. Time variation in the state variables. Panel A shows the extracted time variation in the activity rate V_t from the model estimated jointly to the caps and swaptions markets. Panel B shows the corresponding activity rate to the jump component ν_t in the LIBOR forward rate. Data are weekly (Wednesday) spanning our entire data sample August 8, 2007 to August 11, 2010, in total 158 weeks.

swiss:finance:institute

c/o University of Geneva
40 bd du Pont d'Arve
1211 Geneva 4
Switzerland

T +41 22 379 84 71
F +41 22 379 82 77
RPS@sfi.ch
www.SwissFinanceInstitute.ch